

# Atomic interferometer measurements of Berry's and Aharonov-Anandan's phases for isolated spins $S > \frac{1}{2}$ non-linearly coupled to external fields

Marie-Anne Bouchiat

*Laboratoire Kastler-Brossel, CNRS, UPMC, École Normale Supérieure, 24, rue Lhomond, 75005 Paris France,*

Claude Bouchiat

*Laboratoire de Physique Théorique de l'École Normale Supérieure,  
CNRS, UPMC, 24, rue Lhomond, 75005 Paris France.*

(Dated: May 31, 2021)

In a recent article we have studied the peculiar features of the Berry and Aharonov-Anandan's geometric phases for isolated spins  $S \geq 1$ . We have assumed that they are submitted to a dipole and quadrupole coupling to external  $\mathbf{E}$  and  $\mathbf{B}$  fields with the mild restriction  $\mathbf{E} \cdot \mathbf{B} = 0$ . This implies discrete symmetries leading to remarkable simplifications of the geometry and algebra involved. The aim of the present work is to describe realistic proposals, within the realm of Atomic Physics, for the verification of some of our most significant theoretical predictions. There are several challenges to be overcome. For alkali atoms, most commonly used in atomic interferometers, the only practical way to generate quadrupole coupling, with a strength comparable to the dipole one, is the ac Stark effect induced by a nearly resonant light beam. One has then, to face the instability of the "dressed" atom hyperfine (hf) level, candidate for our isolated spin. One deleterious effect is the apparition of an imaginary part in the quadrupole to dipole coupling strength ratio,  $\lambda$ . Fortunately we have found a simple way to get rid of  $\Im(\lambda)$  by an appropriate detuning. We are left with an unstable isolated spin. This implies an upper bound to the quantum cycle duration  $T_c$ . In the case of the Berry's phase,  $T_c$  has a lower bound coming from the necessity of keeping the non-adiabatic corrections below a predefined level. We have found a compromise in the case of the  $F = 2, m = 0$   $^{87}\text{Rb}$  ground state hf level. This is our candidate for the measurement of the somewhat "exotic" Berry's phase acquired by the  $S = 2, m = 0$  state at the end of a quantum cycle involving a rotation of  $\pi$  of the  $\mathbf{E}$  field - in practice the linear polarization of the dressing beam - about the  $\mathbf{B}$  field direction. We have found a way to implement in a Ramsey-type interferometric measurement the procedures aiming at a control of the non-adiabatic corrections, as described in details in our previous theoretical article. A numerical simulation of our experimental proposal shows that a 0.1% accurate determination of Berry's phase, free of non-adiabatic corrections, can be achieved. Measurements could be considered also for cold  $^{52}\text{Cr}$  chromium atoms with  $S = 3$ , where values of  $\lambda \simeq 1$  can be obtained with an instability smaller than in the  $^{87}\text{Rb}$  case, due to a more favourable spectroscopic structure. The  $F = 1, m = 1$  hf level of the  $^{87}\text{Rb}$  ground state offers the opportunity to extend the measurement of Aharonov-Anandan's phases beyond the case  $S = \frac{1}{2}$ . We construct, using "light shift", the Hamiltonian  $H_{\parallel}(t)$  generating a closed circuit in the density matrix space which satisfies at any time the "parallel transport" condition, thus making the quantum cycle free from the adiabaticity condition. We also consider the case of half-integer spins (*e.g.*  $^{201}\text{Hg}$ ,  $^{135}\text{Ba}$  and  $^{137}\text{Ba}$ ), with their own specific features. We show how the difference of Berry's phases for states  $S = \frac{3}{2}$  and  $S = \frac{1}{2}$ , with  $m = \frac{1}{2}$ , can be exploited to achieve an holonomic maximum entanglement of three Qbits.

PACS numbers: 03.65.Vf, 42.50.Hz, 03.75.Dg, 37.25.+k, 03.67.Bg

## I. INTRODUCTION

In a separate paper [1] we have presented a theoretical study of the Berry's phases generated by cyclic evolution of isolated spins of arbitrary large values. It was assumed that the spins interact non-linearly with time-dependent external electromagnetic fields (possibly effective ones) via the superposition of a dipole and a quadrupole coupling. We have made the assumption that the two effective fields are orthogonal, a mild restriction but with many advantages. It implies several discrete symmetries of the spin Hamiltonian which simplify considerably the geometry and the algebra. Our purpose here, is to suggest atomic physics experiments to observe the original features of the Berry's phases that we predicted, but are

still not revealed.

In the present work we shall be mainly concerned by the adiabatic quantum cycles within a given time interval. They are generated by a Hamiltonian depending on a set of parameters assumed to be a system of coordinates for a differential manifold. In this way, an adiabatic quantum cycle generates a mapping of a close circuit drawn upon the parameters space onto a closed loop upon the density matrix space. The Berry's phases can then be viewed as the geometric phases associated with this particular class of quantum cycles.

The quantum mechanics postulates imply that Berry's phases can be written as Bohm-Aharonov loop integrals. The associated Abelian gauge field is acting within the space formed by the external parameters of the Hamiltonian governing the quantum adiabatic cycles. In the

case of a non-linear Hamiltonian, involving both dipole and quadrupole couplings with the  $\mathbf{B}$  and  $\mathbf{E}$  fields satisfying the condition  $\mathbf{E} \cdot \mathbf{B} = 0$ , the parameter space becomes isomorphic to the two-dimension (2D) complex projective space,  $\mathbf{CP}_2$ . Quite remarkably,  $\mathbf{CP}_2$  can be identified with a solution of the Einstein equations in the 4D real Euclidian curved space [2, 3]. This kind of solutions appears in Quantum Theory of Radiation under the name of ‘‘Gravitational Instantons’’ [4]. This strongly contrasts with the magnetic dipole case where the parameter space is the familiar 2D sphere, and the Berry’s phase gauge field the vector potential of a magnetic monopole, written in spherical coordinates. When both the dipole and the quadrupole couplings are present, the Berry’s phase gauge field has a more complex structure, even for quantum cycles lying upon  $\mathbf{CP}_2$  subspaces isomorphic to the 2D sphere [29]. The observation of these non-trivial geometry features, predicted by Quantum Mechanics, deserves, in our opinion, a precise experimental investigation. We suggest interferometric measurements, involving light-shifted  $^{87}\text{Rb}$  hyperfine sub-levels, in order to exhibit these somewhat exotic quantum effects.

It is quite natural to ask: how can one get from experiment the geometric phase associated with a quantum cycle of the density matrix  $\rho$ , since, by definition,  $\rho$  is phase independent? The answer is to be found within the Superposition Principle of Quantum Mechanics: any linear combination of two quantum states  $|\Psi_1\rangle$  and  $|\Psi_2\rangle$  relative to a given quantum system,  $|\Psi_{12}\rangle = c_1|\Psi_1\rangle + c_2|\Psi_2\rangle$  is an accessible state for the system. In the present atomic physics context, such a construction will be achieved via the interaction of the system with specific classical radio-frequency fields, using so-called Ramsey pulses [5]. The density matrix associated with  $|\Psi_{12}\rangle$  is  $\rho_{12} = |\Psi_{12}\rangle\langle\Psi_{12}| = |c_1|^2\rho_1 + |c_2|^2\rho_2 + \Delta\rho_{12}$ . The crossed contribution:  $\Delta\rho_{12} = c_1 c_2^* |\Psi_1\rangle\langle\Psi_2| + h.c.$  contains all the information needed to obtain the difference of the geometric phases acquired by the states  $|\Psi_1\rangle$  and  $|\Psi_2\rangle$  during an adiabatic quantum cycle. We will discuss experimental schemes, where the geometric phase acquired by one state of the superposition will be known *a priori* to be zero, and one measures then directly the phase acquired by the second state *modulo*  $2\pi$ .

It is not possible to summarize here all the work stimulated by the original contributions of M. Berry, B. Simon, Y. Aharonov, D. Bohm and J. Anandan [6–9]. We refer the reader to review papers [11, 25], pedagogical presentations [12–14], several recent spin-off in quantum computing [15, 16] and the possible impact on precision measurements [17–20]. But we have found in the literature only few papers dealing with the Berry’s phase for a spin submitted to a time-varying quadratic interaction [21, 24, 25]. The authors deal with the nuclear quadrupole resonance (NQR) spectra in a magnetic resonance experiment involving a rotating sample. However, they assume the absence of any magnetic interaction and this leads to level-degeneracy. Thus, the problem is generalized to the adiabatic transport of degenerate states.

In such a situation, the geometric phase is replaced by a unitary matrix given by the Wilson loop integral of a  $SU(n)$  non-abelian gauge potential where  $n$  is the dimension of the eigenspace associated with a given degenerate quantum level [22, 23]. This makes an important difference with respect to the conditions considered here, as well as in our theoretical work where level degeneracy was required to be absent.

Throughout this paper we shall deal with a set of quadratic spin Hamiltonians

$$H(\mathbf{B}(t), \mathbf{E}(t)) = \gamma_S \mathbf{S} \cdot \mathbf{B}(t) + \gamma_Q (\mathbf{S} \cdot \mathbf{E}(t))^2, \quad (1)$$

containing a Zeeman shift produced by a magnetic field  $\mathbf{B}(t)$  (real or effective) and a quadratic Stark shift produced by an electric field  $\mathbf{E}(t)$  (mainly effective). The non-linear spin coupling is responsible for new physical features becoming apparent for  $S > 1$ .

A crucial step, in the confrontation of the theoretical results with experiments, was to realize that, rather than the standard dc-Stark effect, the ac-Stark shifts, induced by a nearly resonant linearly polarized laser beam, were the proper tools to generate an effective  $\mathbf{E}$  field. Samples of cold alkali atoms or trapped alkali-like ions appear then as good candidates for the observation of the Berry’s phases induced by non-linear coupling. Our spin system  $\mathbf{S}$  is identified with the total angular momentum  $\mathbf{F}$  acting upon a given hyperfine (hf) sub-level of an alkali atom ground state.

Our method relies upon the second-order ac Stark shifts involving optical frequencies nearly resonant for the transitions  $S_{1/2,F} \rightarrow P_{1/2,F'}$ , with an appropriate choice of the detunings [26]. This would then allow to use the hyperfine ground state sub-levels of rubidium and cesium isotopes to simulate isolated spin systems with  $S$  having integer values between one and four. In addition, the laser frequency can be tuned for making one of the hyperfine sub-level insensitive to the laser field. It will then provide an absolute phase reference for the second hyperfine sub-level which is performing a quantum cycle.

However, the method of ac-Stark shift to construct the quadratic coupling, presents one drawback. Under the effect of irradiation by the light field, the hyperfine ground state sub-level used to simulate our spin system will acquire a finite decay rate. This puts an upper limit upon the time available for performing one quantum cycle and detecting the associated phase shift. There are atomic species for which this detrimental effect is much less severe. For instance the  $^{201}\text{Hg}$  mercury isotope, (and alkali-earth-like atoms with half-integer nuclear spin) have a spectroscopic structure more favourable for this purpose. It appears that  $^{52}\text{Cr}$  chromium atoms with a spin 3 of purely electronic origin could provide suitable and especially interesting candidates.

The derivation of the Berry’s phase requires the validity of the adiabatic approximation. This means that to perform a valid measurement, one must exert a very tight control upon the non-adiabatic corrections, which are governed by the Hamiltonian-parameter velocities.

This problem is particularly crucial, here, because of the instability introduced by the ac Stark shift in our spin system. It is addressed in great detail in our previous theoretical work [1]. We have proposed explicit solutions for approaching the adiabaticity criterion while ramping up the  $\mathbf{E}$  field and applying the angular rotation speed of the periodic Euler angles. We have given definite procedures for reducing, eventually suppressing non-adiabatic corrections of various origins.

As two examples of the new features of the Berry's phases generated by the quadratic Hamiltonian let us consider two particular set of adiabatic cycles within the time interval  $0 \leq t \leq T_c$ .

i) The  $\mathbf{B}$  field is precessing around a fixed axis, while the  $\mathbf{E}$  field (orthogonal to  $\mathbf{B}$ ) is lying within the rotating plane defined by  $\mathbf{B}$  and the rotation axis.

ii) The direction of the  $\mathbf{B}$  field is fixed and the orthogonal  $\mathbf{E}$  field is rotating around  $\mathbf{B}$  by an angle  $\alpha(t)$  with the boundary condition  $\alpha(T_c) - \alpha(0) = \pi \text{ modulo } \pi$ . Performing an "adiabatic" increase of the  $\mathbf{E}$  field starting from a null value, we have obtained in [1] a mathematical form of the Berry's phase relative to cycle i) which looks superficially similar to that of a linear Hamiltonian. However, there is one *significant difference*: the contribution involving the cosine of the B field tilt angle is no longer proportional to the magnetic quantum number  $m$  whatever the spin value, but instead to the spin polarization along the  $\mathbf{B}$  field. In addition, *a new contribution* to the Berry's phase is generated at the end of the cycle ii). It is given by the spin polarization times the rotation angular speed  $\dot{\alpha}(t)$  integrated over the  $0 \leq t \leq T_c$  interval. A striking case is that of  $m = 0$  for a spin larger than 1, the usual Berry's phase generated by the linear Hamiltonian has a null value, while the one generated by the quadratic Hamiltonian of Eq. (1) is non-vanishing and increases with the magnitude of  $\mathbf{E}$  up to a maximum growing with the value of the spin (especially when it is an even integer). Our aim, here, is to define the precise experimental procedure required for the observation of such new features of the Berry's phase, emerging from our previous work [1].

We have already underlined that the  $\mathbf{E}, \mathbf{B}$  field orthogonality condition endows our problem with important symmetry properties and that it also makes the parameter space isomorphic to  $\mathbf{CP}^2$ , but in addition, for the special case of spin one, this condition implies the isomorphism of the density matrix with the parameter spaces. Thus, the Berry's phase generated by the quadratic spin Hamiltonian was found to be mathematically identical to the Aharonov-Anandan (AA) phase using an appropriate parametrization of  $\mathbf{CP}^2$ . However, the physical contents are in general different, since, in contrast to the Berry's phase, the AA phase is not restricted to *adiabatic* quantum cycles. This case was previously discussed theoretically by C. Bouchiat and G.W. Gibbons [28] and C. Bouchiat [29]. Using cold  $^{87}\text{Rb}$  atoms in the hf state  $F = 1$  experiencing a quadratic ac Stark shift, we propose here to perform an experimental comparison between the

AA and Berry's phase in different adiabatic and non-adiabatic regimes, first, to verify, within the adiabatic approximation, the identity between Berry's and AA phases for appropriate parametrization and second, to observe the difference in their behaviour when the adiabatic approximation begins to fail. We show how a geometric phase equal to Berry's should be still obtained by performing a quantum cycle within the condition of "parallel transport",  $\text{Tr}(\rho(t) H_{\parallel}(t)) = 0$ , *without any constraint upon the time derivatives of the physical observables*. We shall discuss the realization of measurements of this kind with  $^{87}\text{Rb}$  atoms in their hf state  $F = 1$ , showing interest for the fast accomplishment of elementary operations in quantum processing. *For spins larger than one*, the Berry's phase relative to the Hamiltonian considered in this work loses the identity with the AA phase, which involves now closed circuits drawn upon larger projective complex planes  $\mathbf{CP}^{2S}$ .

Finally, as an additional support to the present experimental program, we would like to point out that it may have other significative physical spin-off. A first simple suggestion would be to stop midway the adiabatic cycle described in the present paper. For an appropriate choice of the Hamiltonian parameters, one obtains an example of "coherent spin-squeezed" states [30–32]. A second example relies upon the non-trivial dependence upon  $\mathbf{S}^2$  of Berry's phases of the present paper, in contrast with the dipole case where Berry's phase is proportional to the magnetic quantum number  $m$  whatever  $S$ . This property is the basic ingredient used to perform an "holonomic entanglement" of  $N$  non-correlated spins  $1/2$  (or  $Q$  bits) having a fixed number of spins "down". The corresponding vector state can be written as a linear combination of the eigenstates  $\Psi_{S,M}^i$  of  $\mathbf{S}^2$  and  $S_z$  where  $\mathbf{S} = \sum_{i=1}^N \mathbf{s}_i$  is the total spin operator. Despite the fact that a given eigenvalue of  $\mathbf{S}^2$  may appear several times among them, the states  $\Psi_{S,M}^i$  can always be chosen to have different symmetry properties upon the permutations of the  $N$  spins, insuring their orthogonality. If we assume that in formula (1)  $\mathbf{S}$  stands for the total spin operator introduced above, the corresponding Hamiltonian  $H_N(t)$  is clearly invariant upon all the permutations of the  $N$  spins. As a consequence, it acts upon the states  $\Psi_{S,M}^i$  as if they were isolated spin systems. At the end of the Berry' cycle, they acquire a phase depending upon their  $S$  values. This implies an entanglement of the initially non-correlated  $N$  spin states [1]. In the two particular examples with  $N = 3, 4$  and one spin down, *i.e*  $M = S - 1$ , the parameters of the cycle can be chosen in order to achieve a maximum entanglement. (The simplest non-trivial example,  $N = 3$ , is discussed in the Appendix).

Sec.II is a summary of our theoretical work [1] which presents the remarkable properties of Berry's phases acquired by an arbitrary spin, non-linearly coupled, at the end of a closed adiabatic quantum cycle. We also remind different procedures for keeping the non-adiabatic corrections below a predetermined level. In Sec.III, the

expression of the quadratic spin Hamiltonian Eq. (1) is derived in terms of the experimental parameters for alkali atoms lighted up with a laser beam close to resonance. We present new possibilities offered by cold  $^{52}\text{Cr}$  chromium atoms which are now available. Sec.IV describes a Ramsey type interferometry measurement of Berry's phase, free of any non-adiabatic correction, acquired by the  $F = 2, m = 0$  hf substate of  $^{87}\text{Rb}$ , at the end of a quantum cycle induced by an  $\mathbf{E}$  field rotating around a fixed  $\mathbf{B}$  field. Sec. V underlines the peculiar features of half-integer spin Berry's phases, also yet non-observed. They are illustrated by the case of spins three-half, where two types of measurements look possible. One involves  $^{201}\text{Hg}$  atoms (or other alkali-earth-like odd isotopes), the second a nuclear quadrupole resonance experiment on a uniaxial crystal placed in a magnetic field. Sec.VI deals with the particular case  $S=1$ . We give a method to achieve parallel transport on  $^{87}\text{Rb}$   $F = 1$  atoms and perform an experimental comparison between Berry's and AA phases. Finally Sec.VII is a summary of our work and possible development.

## II. SUMMARY OF BERRY'S PHASE THEORY FOR ARBITRARY SPINS NON-LINEARLY COUPLED TO EXTERNAL FIELDS

Throughout this paper, we make two important assumptions, first *the two spin couplings*, linear and quadratic, can be made of *comparable magnitudes*, second *the effective fields  $\mathbf{B}$  and  $\mathbf{E}$  are orthogonal*.

### A. Symmetry properties of the non-linear spin Hamiltonian. Physical implications

In order to exhibit the geometric structure of the Hamiltonian  $H(\mathbf{B}, \mathbf{E})$ , let us introduce the rotation  $R(t)$  mapping the coordinate trihedron  $(\hat{x}, \hat{y}, \hat{z})$  upon the trihedron defined by the directions of the  $\mathbf{B}, \mathbf{E}$  fields:  $R(t) = \mathcal{R}(\hat{z}, \varphi(t))\mathcal{R}(\hat{y}, \theta(t))\mathcal{R}(\hat{z}, \alpha(t))$ , where  $\mathcal{R}(\hat{u}, \chi(t))$  is standing for the rotation of angle  $\chi(t)$  around the unit vector  $\hat{u}$ . A very convenient mathematical tool is the unitary transformation:  $U(R(t)) = \exp -\frac{i}{\hbar}S_z\varphi(t) \exp -\frac{i}{\hbar}S_y\theta(t) \exp -\frac{i}{\hbar}S_z\alpha(t)$ , which performs the rotation of the spin operator:  $U^\dagger(R(t))\mathbf{S}U(R(t)) = R(t) \cdot \mathbf{S}$ . This rule allows us to write:  $H(\mathbf{B}, \mathbf{E}) = \gamma_S B \hbar U(R(t))\mathcal{H}(\lambda)U^\dagger(R(t))$ , with  $\mathcal{H}(\lambda) = S_z \hbar^{-1} + \lambda S_x^2 \hbar^{-2}$ . Taking aside the energy scale  $\gamma_S B \hbar$ , the dimensionless parameter  $\lambda = \hbar \gamma_Q E^2 / (\gamma_S B)$ , combined with the Euler angles  $\theta, \varphi, \alpha$  provides a set of dimensionless parameters for  $H(\mathbf{B}, \mathbf{E})$ , which could serve as coordinates for the  $\mathbf{CP}^2$  projective space.

The eigenstates of  $\mathcal{H}(\lambda)$ ,  $\hat{\psi}(\lambda, m)$  are labeled with a "magnetic" number  $m$  by requiring that their analytical continuation towards  $\lambda = 0$  coincide with the angular momentum eigenstates  $|S, m\rangle$ . Similarly, the associated eigenenergies  $\mathcal{E}(\lambda, m)$  satisfy the boundary condi-

tion:  $\mathcal{E}(0, m) = m$ .

Thanks to the constraint  $\mathbf{E} \cdot \mathbf{B} = 0$ ,  $\mathcal{H}(\lambda)$  has several discrete symmetries, leading to important physical consequences [1].

- *a.* The "m" parity  $(-1)^{S-m}$ , associated with a  $\pi$ -rotation around  $\hat{z}$ , is a good quantum number for  $\mathcal{H}(\lambda)$ . As a consequence,  $\mathcal{H}(\lambda)$  cannot mix angular momentum states  $|S, m\rangle$  with opposite "m" parities and it can be expressed, within the angular momentum basis, as the direct sum of two matrices acting respectively upon the states with even and odd  $m$  parity:  $\mathcal{H}(\lambda) = \mathcal{H}_{\text{even}}(\lambda) \oplus \mathcal{H}_{\text{odd}}(\lambda)$ .
- *b.*  $\mathcal{H}(\lambda)$  obeys under the rotation  $\mathcal{R}(\hat{x}, \pi)$  the transformation law:  $\mathcal{H}(\lambda) \rightarrow -\mathcal{H}(-\lambda)$ . Since the rotation  $\mathcal{R}(\hat{x}, \pi)$  flips the spin component along the  $z$  axis, one gets the symmetry relation:  $\mathcal{E}(m, \lambda) = -\mathcal{E}(-m, -\lambda)$ .
- *c.* The invariance of  $\mathcal{H}(\lambda)$  upon the rotation  $\mathcal{R}(\hat{z}, \pi)$  implies that the quantum average of  $\mathbf{S}$  relative to the vector state  $\hat{\psi}(\lambda, m)$  lies along the  $z$  axis:  $\langle \hat{\psi}(\lambda, m) | \mathbf{S} | \hat{\psi}(\lambda, m) \rangle = \hbar p(m, \lambda) \hat{z}$  where  $p(m, \lambda)$  will be referred as the polarization of the spin state. Remembering that the unit vector  $\hat{z}$  is taken along the  $\mathbf{B}$  field, one gets for the following quantum spin average:  $\langle \mathbf{S} \rangle = \hbar p(m, \lambda) \mathbf{B}/B$ .
- *d.* The last invariance is somewhat more subtle than the three others since it involves the antiunitary transformation associated with the product of the time reversal by the space reflection with respect to the  $xy$  plane. It implies that  $\hat{\psi}(\lambda, m)$  can be represented by a real vector. As we shall see this result has non-trivial physical consequences.

The eigenvalues of  $H(\mathbf{B}, \mathbf{E})$  together with the associated eigenvectors  $\Psi(m, \lambda)$  can be written as:  $E(m, B, E) = \gamma_S B \mathcal{E}(m, \lambda)$ ;  $\Psi(m, \lambda, t) = U(R)\hat{\psi}(m, \lambda)$ . The spin quantum average relative to  $\Psi(m, \lambda)$  is along the  $\mathbf{B}$  direction:  $\langle \mathbf{S} \rangle = \hbar p(m, \lambda) \mathbf{B}/B$ . Using the Hellmann-Feynmann theorem,  $p(m, \lambda)$  is obtained by taking the partial derivative of the energy  $E(m, B, E)$  with respect to  $\gamma_S B$ :  $p(m, \lambda) = \mathcal{E}(m, \lambda) - \lambda \frac{\partial \mathcal{E}(m, \lambda)}{\partial \lambda}$ . Note that  $p(m, \lambda)$  obeys under the reversal of  $\lambda$  the same symmetry law as  $\mathcal{E}(m, \lambda)$  derived in •*b.* The curves representing the variations of  $\mathcal{E}(m, \lambda)$  and  $p(m, \lambda)$  versus  $\lambda$  for  $S = 2, 3$  and 4 are displayed in Fig. 1 of our previous paper [1].

### B. A sketchy derivation of Berry's phases for adiabatic cycles governed by $H(\mathbf{B}, \mathbf{E})$

We have now all the necessary ingredients to sketch the derivation of the Berry's phase using the instantaneous eigenfunctions  $\Psi(m, \lambda, t)$  given in the previous subsection. Our starting point is the standard formula:

$$\beta(m) = \int_0^T dt \langle \Psi(m, \lambda, t) | i \frac{\partial}{\partial t} \Psi(m, \lambda, t) \rangle + \phi(m)$$

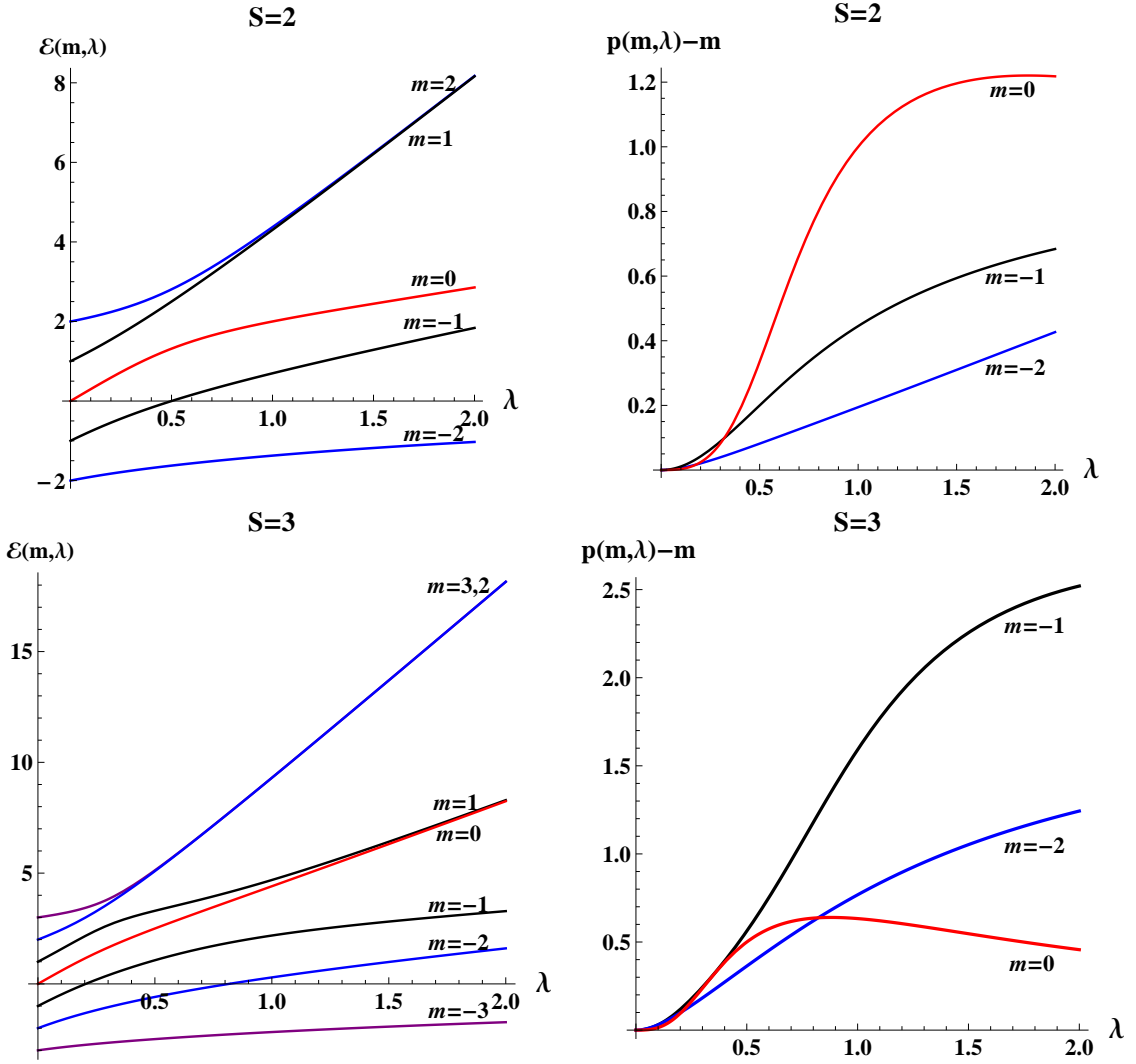


FIG. 1: (Color online) Reduced energies  $\mathcal{E}(m, \lambda)$  (left-hand) and gauge field components  $A_\alpha = p(m, \lambda) - m$  (right-hand) versus  $\lambda$  for  $S = 2$  and  $S = 3$ , for selected  $m$ -values relevant for the discussion presented in subsec. 2.C. Intersection of the energy curves with the vertical axis indicates the eigenvalues  $m$  of  $S_z$  for  $\lambda = 0$ . For  $\lambda > 0$  remarkable effects appear for  $S = 2$ ,  $m = 0$  and for  $S = 3$ ,  $m = -1$ . In both cases this occurs in a range of Stark to Zeeman coupling ratios where the levels are well separated.

$$\text{with } \phi(m) = \arg(\Psi(m, \lambda(0), T) / \Psi(m, 0, \lambda(0))), \quad (2)$$

where we have used the fact that  $\lambda$  is a non periodic parameter:  $\lambda(T) = \lambda(0)$ . Inserting  $\Psi(m, \lambda, t) = U(R)\hat{\psi}(m, \lambda)$ , the time integral contribution can be rewritten as:  $\gamma(m) = \int_0^T dt i \hbar \langle \hat{\psi}(m, \lambda) | (\frac{\partial}{\partial t} + U^\dagger(R) \frac{\partial}{\partial t} U(R)) \hat{\psi}(m, \lambda) \rangle$ . Since  $\hat{\psi}(m, \lambda)$  is a normalized real vector, the first term inside the parenthesis vanishes. In the second term, the operator  $i \hbar U^\dagger(R) \frac{\partial}{\partial t} U(R)$  is a standard group theory object which can be expressed under the canonical form:  $i \hbar U^\dagger(R) \frac{\partial}{\partial t} U(R) = \vec{\omega}(t) \cdot \mathbf{S}$ , where  $\vec{\omega}(t)$  is a real vector. Its three components are linear functions of the time derivatives of the Euler angles. Their explicit expressions can be found in references [1, 28]. Using •c, one sees immediately that only the  $z$ -component  $\omega_z = \cos(\theta)\dot{\phi} + \dot{\alpha}$

does contribute:  $\gamma(m) = \int_0^T dt p(m, \lambda) (\cos(\theta)\dot{\phi} + \dot{\alpha})$ . The calculation of  $\phi(m)$  is performed in details in references [1]. It is greatly simplified by the particular features of the expansion of  $\hat{\psi}(m, \lambda)$  over the angular momentum eigenstates resulting from properties •a. and •d, which lead to :  $|\hat{\psi}(m, \lambda(0)) = \sum_{|m-2n| \leq S} C_{m,n}(\lambda(0)) |S, m-2n\rangle$ . The sum runs upon states of the same  $m$ -parity and the coefficient  $C_{m,n}$  are real numbers. One can factorize out from  $U(R(T))U^\dagger(R(0))$  the operator giving the phase shift  $\phi(m)$ :  $U_\phi = \exp(-\frac{i}{\hbar} S_z (\varphi(T) - \varphi(0) + \alpha(T) - \alpha(0)))$ . Remembering the quantum cycle boundary conditions:  $\varphi(T) - \varphi(0) = 2n_\varphi \pi, \alpha(T) - \alpha(0) = n_\alpha \pi$ , one sees that the effect of  $U_\phi$  upon the terms of the expansion of  $\hat{\psi}(m, \lambda(0))$  is just to multiply them by the same phase

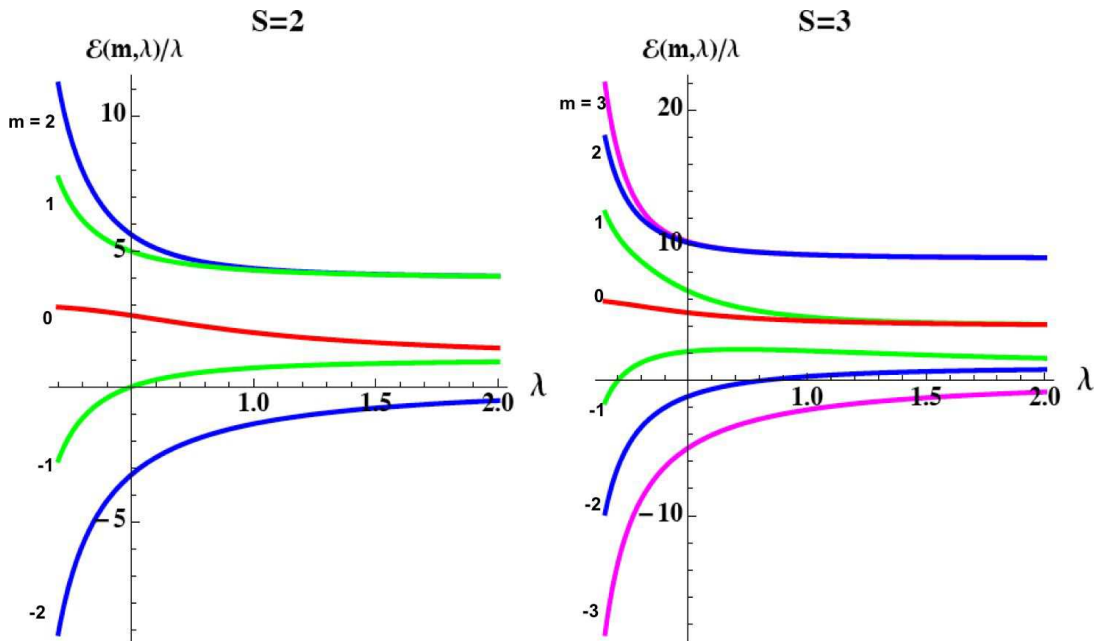


FIG. 2: (Color online) Plot of  $\mathcal{E}(m, \lambda)/\lambda$  within the interval  $0.1 \leq \lambda \leq 2$ , allowing us to clarify the rearrangement of  $2S + 1$  non-degenerate levels for  $\lambda \ll 1$ , into  $S$  degenerate doublets with  $\mathcal{E}(m, \lambda)/\lambda \simeq \mu^2$  in the limit  $\lambda \gg 1$ ,  $\mu$  being an integer such that  $-S \leq \mu \leq S$ . Starting from the even-odd (or odd-even) pair:  $\{\mathcal{E}(S, \lambda)/\lambda, \mathcal{E}(S-1, \lambda)/\lambda\}$ , one sees clearly that the pair converges, *without crossing*, towards the degenerate doublet with:  $\mathcal{E}(S, \lambda)/\lambda \simeq \mathcal{E}(S-1, \lambda)/\lambda \simeq S^2$ . The next lower pair will end as the degenerate doublet having the energy  $\simeq \lambda(S-1)^2$  and so on, until one reaches the isolated level with  $\mu = -S$ . It has no other possibility than to converge to the non degenerate level with  $\mu^2 = 0$ . The fact that there is no level crossing for finite values of  $\lambda$  follows from the very simple mathematical structure of the Hamiltonian  $\mathcal{H}(\lambda)$ . Indeed, any modification of its symmetry properties, is excluded until one reaches the limit  $\lambda \rightarrow \infty$ .

factor:  $\exp -im(\varphi(T) - \varphi(0) + \alpha(T) - \alpha(0))$ . In this way one obtains  $\phi(m) = -\int_0^T m(\dot{\varphi}(t) + \dot{\alpha}(t)) dt$ .

We arrive at our final expression for the Berry's phase in terms of a loop integral along a closed circuit drawn upon the parameter space  $\mathbf{CP}^2$ :

$$\begin{aligned} \beta(S, m) &= \oint_c A_\varphi(S, m, \lambda) d\varphi + A_\alpha(S, m, \lambda) d\alpha, \\ A_\varphi(S, m, \lambda) &= p(S, m, \lambda) \cos \theta - m, \\ A_\alpha(S, m, \lambda) &= p(S, m, \lambda) - m. \end{aligned} \quad (3)$$

In the writing, we have stressed the two new physical features introduced by the quadrupole spin coupling: first, the Aharonov Bohm-like integral now involves a two-component Abelian gauge field  $(A_\varphi, A_\alpha)$  instead of a single one, second, it now exhibits a strong dependence upon the value of  $\mathbf{S}^2 = \hbar^2 S(S+1)$ , in contrast with the dipole case where the Berry's phase depends only upon  $m$ . The latter effect reflects the fact that the polarization  $p(S, m, \lambda)$  has a simple linear relation with  $\mathcal{E}(m, \lambda)$ . These eigenenergies are given by the roots of two polynomials having respectively the degree  $S+1$  and  $S-1$  and coefficients which are  $\lambda$  monomials. As a consequence, for  $S \geq 4$  the eigenenergies are given by transcendental functions of  $\lambda$ .

### C. Physical implications of the S-dependence of Berry's phases generated by $H(\mathbf{B}, \mathbf{E})$

For integer spin values, remarkable effects are predicted when Berry's cycles have as initial state the angular momentum eigenstate  $|S, 0\rangle$ , corresponding to an initially vanishing polarization  $p(S, 0, 0) = 0$ . If no  $\mathbf{E}$  field is applied during the cycle, the polarization keeps its null value all along the cycle and one recovers the well known result  $\beta(S, 0, 0) = 0$ . However, if the  $\mathbf{E}$  field intensity is ramping up to a maximum before  $\alpha$ -rotation starts and returning to a null value when it stops, the initial state is mixed with states  $|S, m\rangle$  with  $m = \pm 2n$  ( $n$  is an integer  $\leq S/2$ ). For  $S > 1$  a finite polarization  $p(S, 0, \lambda)$  appears to third order in  $\lambda$  given by  $p(0, \lambda) = \frac{1}{8}\lambda^3 S(S+2)(S^2-1)(1 + \mathcal{O}(\lambda^3))$ . Finite values for the gauge field  $(A_\varphi, A_\alpha)$  are then generated.

In the following we concentrate upon the cycles where  $\alpha$  and  $\lambda$  are the sole varying parameters. As a consequence, only the gauge field component  $A_\alpha$  is relevant. We have displayed in Figure 1 the variations with  $\lambda$  of  $\mathcal{E}(S, m, \lambda)$  for  $S = 3$  and 2 with  $m = 0, \pm 1, \pm 2$ , together with that of the gauge field  $A_\alpha(S, m, \lambda)$  for  $m = 0, -1, -2$ . One sees clearly that the relevant energy levels are well separated. The magnitude of  $A_\alpha(S, m, \lambda)$  is remarkably large for  $S = 2, m = 0$ , in strong contrast

with the case of a linear spin Hamiltonian. We note that  $A_\alpha(S, 0)$  is smaller for  $S = 3$ . For  $|\lambda| < 1$ , this follows from the fact that the term  $\propto \lambda^5$  has a large coefficient which changes its sign with the parity of  $S$ . For  $m = -1$ , the largest value of  $A_\alpha(S, -1)$  occurs for  $S = 3$ . We note that  $p(3, -1, \lambda) > 0$  when  $\lambda > 0.7$ . This indicates that the state  $|3, -1\rangle$  is strongly mixed with the states  $|3, m = 1, 3\rangle$  within the range  $.7 \leq \lambda \leq 2$ .

To conclude this subsection, we emphasize that the holonomic entanglement method of  $N > 2$  non-correlated  $\frac{1}{2}$ -spins, described in reference [1], relies upon the fact that Berry's phase has a strong dependence upon  $S$ . A different example is given in Appendix A. In a theoretical note we show how to exploit the difference between Berry's phases for  $S = \frac{3}{2}$  and  $S = \frac{1}{2}$ , with  $m = \frac{1}{2}$ , to perform an holonomic entanglement between three initially non-correlated  $\frac{1}{2}$ -spins.

#### D. A summary of the non adiabatic corrections to Berry's cycles

To perform empirical determinations of the Berry's phase, one must tackle the problem of the non-adiabatic corrections. This question becomes crucial in the experimental situations where the coherence decay time induced by application of the Hamiltonian  $H(\mathbf{B}, \mathbf{E})$  puts constraints on the cycle duration. Shortening the quantum cycle risks to spoil the validity of the adiabatic approximation. In the present context, we have found convenient to study the quantum cycle in the rotating frame attached to the time-varying fields. The Coriolis effect generates an extra magnetic field  $\Delta\mathbf{B}$  which involves a linear combination of the Euler-angles time derivatives. The longitudinal component along the  $\mathbf{B}$  field is the only one which survives when  $\alpha$  is the sole time-dependent Euler angle. The rotating frame Hamiltonian  $\tilde{H}_{//}$  is void of any geometry. As a consequence, the phase shift acquired at the end of the cycle  $\tilde{\phi}(\mathbf{B} + \Delta\mathbf{B})$  is purely dynamical. The laboratory Berry's phase contribution  $\gamma(m)$  is incorporated into the dynamical phase under the form of its first-order contribution with respect to  $\eta = -\Delta B_{//}/B = (\cos\theta \dot{\phi} + \dot{\alpha})/(\gamma_S B)$ . The higher-order terms give all the non-adiabatic corrections associated with  $\dot{\alpha}$  when it is the only varying periodic parameter. We have also shown that the subset of these corrections, odd under a reversal of  $\eta$ , cancel exactly for "magic" values  $\lambda = \lambda^*(\eta)$ , obtained from a polynomial fit performed on the numerical results valid for  $0 \leq \eta \leq 0.5$  (see [1] Sec.V.A)

$$\lambda^*(2, \eta) = 0.838213 - 0.0837823 \eta^2 - 0.0431478 \eta^4 - 0.0231887 \eta^6 - 0.0207986 \eta^8. \quad (4)$$

This cancellation is implemented in the experimental project described in Section IV. The  $\eta$ -even corrections are eliminated by subtracting the phases measured for two "mirror" cycles ( $\eta \rightarrow -\eta$ ). The case of the non-adiabatic corrections induced by the transverse field

$\Delta B_\perp/B$  is somewhat more involved since it introduces a non-trivial geometry and, as a consequence, a Berry's phase contribution to be added to the one coming from the transverse dynamical phase; the results explicated in [1] are not used in the present context.

For the adiabatic approximation to be satisfied, the primary condition is that, at each instant, the spin quantum state is an eigenstate of  $H(\mathbf{B}(t), \mathbf{E}(t))$ . In the above discussion, we have made implicitly the two following assumptions: i) during an Euler angle cycle,  $\lambda(t)$  has a slowly varying value of the order of unity, ii) the initial state of the Euler cycle is obtained by an adiabatic ramping governed by  $\mathcal{H}(\lambda(t)) = S_z + \lambda(t)S_x^2$ , starting from a null value of  $\lambda$  in order to get its desired value for a well defined value of  $m$ . We have shown, by doing explicit calculations, that approaching this ideal "adiabatic ramping" is, in practice, a non-trivial task. The key-parameter which governs the time dependence of the quantum state is the time derivative of  $\lambda$ . A linear increase of  $\lambda(t)$  would be equivalent to a rf pulse with sharp edges, leading to large oscillating non-adiabatic corrections exhibited in ref. [1]. Among several methods [33], a standard procedure to smooth them out is to use a Blackman pulse shape [34]. In the present context, this condition is implemented by taking for  $\lambda(t)$  the following time dependence:  $\lambda(t) = \lambda_0 f(t/\mathcal{T})/f(0)$ , where  $f(s)$  is the Blackman function

$$f(s) = 0.42 - 0.5 \cos(2\pi s) + 0.08 \cos(4\pi s) \quad (5)$$

and  $\mathcal{T}$  the ramping time. The efficiency of the procedure has been illustrated before (see Fig. 5 in [1]).

There is a third assumption implicit in the rotating frame analysis, namely that the adiabatic approximation is valid for the rotating frame Hamiltonian  $\tilde{H}_{//}$ . As will be shown by the theoretical analysis of the experimental project presented in section IV, the adiabatic approximation works beautifully provided one uses also a Blackman-pulse shape for the angular speed,  $\dot{\alpha}(t)$ .

When looking at a plot of  $\mathcal{E}(m, \lambda)/\lambda$  (Fig.2), it appears clearly that there are pairs of states associated with  $m$  values differing by 1 which never cross but become quasi non-degenerate for large values of  $\lambda$ . When one is interested in quantum cycles where only  $\alpha$  and  $\lambda$  are time-dependent this should not affect the results since the Hamiltonian  $H(\mathbf{B}(t), \mathbf{E}(t))$  has no matrix element connecting the  $\Delta m = \pm 1$  states. Nevertheless, when two such levels happen to be close, the spin system becomes particularly sensitive to imperfections which alter the symmetry, as for instance a stray component of the magnetic field orthogonal to  $\mathbf{B}$ .

### III. ATOMIC SIMULATION OF ISOLATED SPINS NON-LINEARLY COUPLED TO EXTERNAL FIELDS.

Since, among cold atoms, alkali are the most frequently studied we first examine what kind of measurement looks

possible in their case. Such a choice is motivated by the fact these systems can be kept in a decoherence-free space for a relatively long time (up to 1 s), if cooled and trapped. But as is well-known, it is very difficult to observe a static quadratic Stark effect on hf sub-levels of alkali ground states, since their electric tensor polarizabilities are strongly suppressed. A tiny effect appears only as the result of a third-order perturbation [35, 36], when the tensor part of the hf interaction is taken into account. The tensor polarizability of Rb  $\alpha_2 \simeq 2$  mHz/(kV/cm)<sup>2</sup> [37], implies that a field of  $\approx 300$  kV/cm would be required to generate a coupling strength of 100 Hz. This makes it unrealistic to use a rotating static E-field to observe the quadratic Berry's phase.

On the other hand one may rely on light shifts [26]. Hereafter, we consider the case of a quadratic coupling induced by linearly polarized light fields which have the advantage, with respect to microwave- or rf-fields, of making the orientation of  $\mathbf{E}$  relative to  $\mathbf{B}$  both precisely adjustable and easily rotated. However, with this method one has to face the problem of instability of the dressed atomic state if one wants to obtain a quadrupole to dipole spin coupling ratio of order 1. This is not straightforward for the ground state hyperfine levels of alkali atoms. In this case, the role of the spin operator  $\mathbf{S}$  is played by the total angular momentum operator  $\hbar\mathbf{F} = \hbar(\mathbf{s} + \mathbf{I})$ , where  $\hbar\mathbf{s}$  and  $\hbar\mathbf{I}$  are the electronic and nuclear spin operators. Actually, we are going to show that the practical realization of the Hamiltonian  $H(\mathbf{B}(t), \mathbf{E}(t))$  required to test the theoretical predictions of this work for  $\lambda \simeq 1$  appears possible for <sup>87</sup>Rb atoms.

Now, in the rapidly expanding family of laser cooled and trapped atoms has appeared the daring alternative of chromium. The great progress achieved in the manipulation of this atom have given rise to a series of beautiful experiments, *e.g.* [38–40]. As a spin  $S = 3$  candidate, it has the advantage of being of pure electronic origin. This makes the instability of the dressed atom no longer a problem. The chromium option is discussed at the end of this section.

#### A. Building quadrupole spin couplings in alkali atoms using the ac Stark effect.

It is known that the application of a light beam close to resonance with one atomic excited state generates light shifts which can simulate the effect of an electric field or a magnetic field [26]. A fictitious  $\mathbf{B}$  field arises if the beam is circularly polarized while a fictitious  $\mathbf{E}$ -field is created by a linearly polarized beam. One might wonder therefore, whether, with a single beam of elliptically polarized light, it would be possible to generate both fictitious electric and magnetic fields satisfying the condition  $\mathbf{E} \cdot \mathbf{B} = 0$ . We consider the case of alkali atoms irradiated by a laser beam nearly resonant with one hf component of the  $nS_{1/2,F} - nP_{1/2,\mathcal{F}}$  transition. The atom-laser coupling responsible for ac Stark shifts - or light shifts - of

the ground state sublevel can be calculated to second order in the atom-radiation field interaction, in the rotating wave approximation (see [26, 27]). If we make the simplifying assumption  $F = \mathcal{F}$ , discussed hereafter, we can use the proportionality between the atomic electric dipole and the angular momentum operators, resulting from the Wigner-Eckart theorem,  $\mathbf{D}/ea_0 = d g_F \mathbf{F}$ , where  $d$  is the  $\Delta m_s = 0$  matrix element of this electric dipole transition in atomic units and  $g_F = 2(F - I)/(I + 1/2)$ . In this case, the light shifts of the hf ground state  $S_{1/2,F}$  can be represented very simply in terms of the effective Hamiltonian

$$\hat{H}_{ls}(F) = \frac{\hbar\Omega^2}{\Delta} g_F^2 \times \left( i\hat{\epsilon}^* \wedge \hat{\epsilon} \cdot F\hat{k} + \frac{1}{2}(\mathbf{F} \cdot \hat{\epsilon}^* \mathbf{F} \cdot \hat{\epsilon} + \mathbf{F} \cdot \hat{\epsilon} \mathbf{F} \cdot \hat{\epsilon}^*) \right), \quad (6)$$

where  $\Omega = d\mathcal{E}/2\hbar$  represents the dipolar coupling of the atom with the laser field. The field magnitude  $\mathcal{E}$  is related to the photon number density by  $\epsilon_0\mathcal{E}^2 = N\hbar\omega/V$  [41, 42] and the complex vector  $\hat{\epsilon}$  of unit norm defines the polarization. For simplicity, we suppose the detuning  $\Delta$  between the laser and the atomic transition frequency,  $\omega_{F,\mathcal{F}}$ , to be small compared to the hf splittings, so that we can consider the contribution of the  $\mathcal{F} = F$  hf line alone,  $\Delta = \omega - \omega_{F,\mathcal{F}}$ . In the next subsection, we shall consider the case where this condition no longer applies. It will turn out that the general form of  $H_{ls}(F)$  is the same but with different coefficients.

A general expression for the elliptical polarization  $\hat{\epsilon}$  of a beam directed along  $\hat{z}$  is:

$$\hat{\epsilon} = \frac{1}{\sqrt{2}}(\cos\delta_e \hat{e}_+ + \sin\delta_e \hat{e}_-) \quad \text{where} \quad \hat{e}_\pm = \frac{\hat{x} \pm i\hat{y}}{\sqrt{2}} \exp(\mp iu), \quad (7)$$

and the angle  $u$  defines the orientation of the ellipse in the  $(x, y)$  plane of polarization.

For  $u = 0$  the expression for  $\hat{H}_{ls}$  obtained after some angular momentum algebra is:

$$\hat{H}_{ls}(F) = \frac{\hbar\Omega^2}{\Delta} g_F^2 \times \left( \cos 2\delta_e F_z + \sin 2\delta_e F_x^2 + (F(F+1) - F_z^2) \frac{1 - \sin 2\delta_e}{2} \right) \quad (8)$$

The first term, linear in  $\mathbf{F}$  involves the circular polarization of the beam, characterized by its helicity  $\xi = \text{Im}\{\hat{\epsilon}^* \wedge \hat{\epsilon} \cdot \hat{k}\} = \cos 2\delta_e$ , while the quadratic contribution  $\propto F_x^2$  involves the linearly polarized intensity. Contrary to a static  $\mathbf{E}$ -field, a laser field can provide a sufficiently strong quadrupolar coupling, for laser power and frequency adjustments lying within convenient limits (see Sec IV). However, because the ac-field is complex, while the dc field is real,  $\hat{H}_{ls}(F)$  actually differs from



the Hamiltonian  $\hat{H}(B, E)$  of Eq.(1) by its last term involving  $F_z^2$ , which cancels out only if the polarization is purely linear, *i.e.*  $\delta_e = \pi/4$ . Although this does not render the light-shift Hamiltonian untractable, one loses the simple symmetry property of the Hamiltonian under the rotation  $\mathcal{R}(\hat{x}, \pi)$  discussed in section II.B. For this reason, to keep our concrete discussion of the theoretical implications as simple as possible, we prefer to choose an experimental situation corresponding to a *hybrid realization* of the field configuration. We shall suppose that  $\mathbf{B} = B\hat{b}$  is a static field, while  $\mathbf{E} = \mathcal{E}\hat{e}$  is a light field, linearly polarized along the direction  $\hat{e}$ , the light beam direction  $\hat{k}$  being taken parallel to  $\hat{b}$ . With this hybrid “**B**-field light-field” Hamiltonian, one can satisfy exactly all the conditions required in ref. [1], by allowing  $\hat{e}$  to rotate around  $\hat{b} \parallel \hat{k}$  at the angular speed  $\dot{\alpha}$ . This hybrid Hamiltonian

$$H_{hyb}(F, t) = \gamma_F \hbar B \mathbf{F} \cdot \hat{b} + \frac{\hbar\Omega^2}{\Delta} g_F^2 (\mathbf{F} \cdot \hat{e})^2, \quad (9)$$

is identical to the Hamiltonian of Eq.(1), if one makes the correspondences

$$\gamma_Q E^2 \hbar^2 \leftrightarrow \frac{\hbar\Omega^2}{\Delta} g_F^2 \quad \text{and} \quad \lambda \leftrightarrow \frac{\Omega^2}{\Delta} g_F^2 / \gamma_F B. \quad (10)$$

We set  $\gamma_F B = g_F \gamma_s B$ , where  $\gamma_s B$  is the Larmor angular frequency of the electron and  $g_F = 2(F - I)/(2I + 1)$ . (Of course the fact that the internal angular momentum  $\mathbf{F}$ , relative to a given hyperfine sub-level, can be treated as an isolated spin implies the reasonable assumption that, for values of  $\lambda \sim 1$ , the Larmor frequency is much smaller than hyperfine splitting.) The use of an ac-light field instead of a static electric field has other advantages besides the magnitude of the Stark coupling. By adjusting the laser detuning, it makes it possible to apply a light field upon a single ground state hf level, the second one remaining spectator and providing the phase reference. The expression for  $\lambda$  also shows there are two independent ways of reversing the sign of the Stark *versus* the Zeeman-coupling: one can reverse either the sign of  $\mathbf{B}$  or else that of the laser detuning.

### B. Solving physical problems raised by the instability of the “dressed” atomic ground state.

The main drawback of the light-shift method for obtaining an effective  $\mathbf{E}$  field, is that it generates an instability of the “dressed” ground state hf sublevel, which is going to simulate our isolated spin system. This instability is best understood within a fully quantized description of the atom interacting with the radiation field. The vector state of the “dressed” atom of interest can be written as:  $|F n S_{1/2}\rangle \otimes |N \hat{e} \omega\rangle$  where  $N$  is the number of photons with energy  $\hbar\omega$  and linear polarization  $\hat{e}$  in the coherent light beam. The light shift is associated with the two successive virtual electromagnetic transitions:  $|F n S_{1/2}\rangle \otimes |N \hat{e} \omega\rangle \Rightarrow |\mathcal{F} n P_{1/2}\rangle \otimes |N - 1 \hat{e} \omega\rangle \Rightarrow$

$|F n S_{1/2}\rangle \otimes |N \hat{e} \omega\rangle$ . More precisely  $|\mathcal{F} n P_{1/2}\rangle$ , for an appropriate detuning, is returning by stimulated emission to the same ground state hf sublevel  $|F n S_{1/2}\rangle$  but with its energy “light-shifted”. An alternative route for the excited state  $|\mathcal{F} n P_{1/2}\rangle$  is to make transitions to ground state hf sublevels, by an energy conserving spontaneous light emission, leading to the infinite set of final states:  $|F' n S_{1/2}\rangle \otimes |N - 1 \hat{e}' \omega'\rangle$  where  $\omega' \neq \omega$  and  $\hat{e}' \neq \hat{e}$ . We see easily that all these final states are orthogonal to the initial “dressed” ground state hf sublevel even if  $F = F'$ . In conclusion, our candidate for an isolated spin system is unstable with a decay rate  $\Gamma_{dec}$  which scales as  $(\Omega^2/\Delta^2)\Gamma_{nP_{1/2}}$ , where  $\Gamma_{nP_{1/2}}$  denotes the spontaneous emission rate of the excited state  $nP_{1/2}$ .

At first sight, since the light-shift involves the inverse of the detuning, while the decay rate scales as the square of this quantity, the choice of large detunings would seem the most appropriate. In fact, this is not so. Indeed, for  $\hbar\Delta$  much larger than the hf frequency splitting of the excited  $P_{1/2}$  state,  $\Delta\mathcal{W}_P$ , the two hf states contribute with nearly equal magnitudes but opposite signs, in such a case the light-induced quadratic spin-coupling vanishes. Therefore, the quadratic coupling is easier to achieve at detunings comparable to  $\Delta\mathcal{W}_P$  for heavy alkali atoms (Rb, Cs) or odd isotopes of alkali-like ions ( $\text{Ba}^+$ ,  $\text{Hg}^+$ ), which have the largest hf splittings. Since the  $P_{3/2}$  hf splitting is smaller than that of  $P_{1/2}$  by a factor 5 in Rb, the light beam should be tuned preferably close to the  $D_1$  resonance line. Detunings of the order of this splitting (0.816 GHz for  $^{87}\text{Rb}$ ) appear to lead to a reasonable compromise solution between decay rate and light shift magnitude (comparable to the Zeeman coupling for a magnetic field in the 0.1-1 mG range, see Sec. IV). For a correct evaluation of  $\lambda$ , we have to include the contributions from both hf  $nP_{1/2}$  levels, with their respective detunings  $\Delta_{F,\mathcal{F}} = \omega - \omega_{F,\mathcal{F}}$ . The explicit formula giving  $\hat{H}_{ls}(F)$  in the case of an alkali ground state hf level  $F$  ( $g_F = 1/(I + 1/2)$ ), lightened by a linearly polarized light beam becomes [41, 42]

$$\begin{aligned} H_{ls}(F) &= \frac{\hbar\Omega^2}{\Delta_{2,1} + i\Gamma_P/2} (\mathbf{1} - g_F^2 (\mathbf{F} \cdot \hat{e})^2) \\ &+ \frac{\hbar\Omega^2}{\Delta_{2,2} + i\Gamma_P/2} g_F^2 (\mathbf{F} \cdot \hat{e})^2. \end{aligned} \quad (11)$$

A remarkable feature of this expression is that, as announced, the two hf  $nP_{1/2}$  levels quadrupole contributions cancel out if the frequency detuning is much larger than the  $nP_{1/2}$  hf splitting,  $\Delta_{2,2} \simeq \Delta_{2,1}$ . In the sum with equal weights of the hf levels numerators the nuclear spin dependence disappears; only remains the effective transition dipole  $\propto \mathbf{s}$ . The instability discussed above has been accounted for by adding to the energy denominator  $+i\Gamma_P/2$ , see ref.[27].

Ignoring for a moment the natural width compared to the detuning, the quadrupole coupling term is given by

an expression identical to Eq. (8). With the definitions:

$$W_{ls} = \hbar \frac{\Omega^2}{\Delta} g_F^2 \quad \text{and} \quad 1/\bar{\Delta} = 1/\Delta_{2,2} - 1/\Delta_{2,1}. \quad (12)$$

we recover the expression of the ‘‘B-field light-shift’’ Hamiltonian:

$$H_{hyb} = \hbar \gamma_F B \mathbf{F} \cdot \hat{\mathbf{b}} + W_{ls} (\mathbf{F} \cdot \hat{\mathbf{e}})^2. \quad (13)$$

deduced from Eq.(9) by substituting  $\bar{\Delta}$  in place of  $\Delta$ .

Let us now turn to the physical effects induced by the imaginary part of the energy denominators. The most dangerous effect involves the imaginary part of the quadrupolar coupling given by the expression

$$g_F^2 \frac{\Gamma_P}{2} \Omega^2 (\mathbf{F} \cdot \hat{\mathbf{e}})^2 \left( \frac{1}{\Delta_{2,1}^2} - \frac{1}{\Delta_{2,2}^2} \right),$$

up to third order in  $\Gamma_P/\Delta$ . This contribution modifies during the quantum cycle the structure of the atomic wave function, which is a linear combination of m-dependent angular momentum states, and hence this invalidates the Berry’s phase derivation of ref. [1]. There is, fortunately, a remedy to this problem. It is to tune the laser frequency midway between resonance with the two hf states as illustrated in the insert of Fig.(3). Then, the imaginary part of  $\lambda$  is vanishing. From the remaining scalar part results a decay rate  $\Gamma_{dec}$  of the dressed atoms,

$$\Delta_{2,1}^2 = \Delta_{2,2}^2 \quad \text{implying} \quad |\Delta_{2,2}| = |\Delta_{2,1}| = 2\pi\Delta\mathcal{W}_P/2, \quad (14)$$

$$\text{and} \quad W_{ls} = \frac{4g_F^2\Omega^2}{2\pi\Delta\mathcal{W}_P}, \quad \Gamma_{dec} = \frac{4\Omega^2}{(2\pi\Delta\mathcal{W}_P)^2}\Gamma_P. \quad (15)$$

From now on, therefore, we shall assume that the laser beam frequency detuning satisfies condition (14) and we rely on Eqs.(13) and (15), to suggest experiments on alkalis. We are left with an ‘‘isolated’’ spin with decay rate  $\Gamma_{dec}$ . For dressed  $^{87}\text{Rb}$  atoms, the spectroscopic parameter governing the instability turns out to be small:

$$\frac{\Gamma_P}{2\pi\Delta\mathcal{W}_P} = 7 \times 10^{-3}, \quad (16)$$

instead of 6 and  $5 \times 10^{-2}$  for  $^7\text{Li}$  and  $^{23}\text{Na}$ . As shown in Sec. IV,  $^{87}\text{Rb}$  thus provides a unique possibility to test Berry’s cycles for  $S = 2$  in the range  $0 < \lambda \leq 1$ .

In the last section we shall be interested in the case of a spin-1 performing a quantum cycle not in the Hamiltonian parameter space but *in the density matrix space* described by the atomic polarization and alignment. The hybrid light-field B-field Hamiltonian considered in this section is adapted to realize a cycle of this kind. The laser beam in this case will be equally detuned from the two hf lines starting from the  $F = 1$  ground state, therefore  $\Delta_{12}^2 = \Delta_{11}^2$ . It is easily verified that all preceding equations remain valid if  $\Delta_{12}$  is changed into  $\Delta_{21}$  and  $\Delta_{22}$  into  $\Delta_{11}$ . We shall need the explicit hybrid Hamiltonian for  $F = 1$ , in the case of an elliptically polarized

laser beam, with ellipticity axes at  $45^\circ$  of the  $x$  and  $y$  axes, *i.e.*  $u = \pi/4$ , and a B-field along the beam:

$$H(W_{ls}, B, \delta_e)/\hbar = W_{ls} \left( \frac{1}{2} \sin(2\delta_e) \{F_x F_y\} - \frac{1}{2} F_z^2 \right) \\ + (W_{ls} \cos(2\delta_e) + \gamma_F B) F_z + W_{ls} \frac{\mathbf{F}^2}{2}, \quad (17)$$

$$\text{with} \quad W_{ls} = \frac{\Omega^2}{2\pi\Delta\mathcal{W}_P}. \quad (18)$$

### C. The special case of $^{52}\text{Cr}$ chromium isotopes with $S=3$

Chromium atoms in their ground state have also  $L = 0$  like alkalis, but they possess a large electronic spin  $S = 3$  and an isotope of 84% natural abundance,  $^{52}\text{Cr}$ , without nuclear spin. The ground state  $^7S_3$  is coupled by dipole transitions to different P-states ( $^7P_{2,3,4}$ ) which have been used for cooling the atoms in an optical dipole trap [38]. With linearly polarized blue lasers suitably detuned from these transitions it is possible to induce Stark shifts proportional to  $m^2$  in the ground state. For instance in the particular case of a small detuning with respect to the  $J$  conserving transition  $^7S_3 \rightarrow ^7P_3$ , equation (9) could be adapted by replacing  $\mathbf{F}$  by  $\mathbf{J}$  and performing some angular momentum algebra. Like in the case of alkalis, detuning and light power have to be adjusted to minimize the instability of the dressed atomic state. However, as in chromium the fine structure of the P-states being about 300 times larger than the hf structure of the alkali P-states, those restrictions are much easier to satisfy. Importantly, it is also much easier to prevent the quadratic coupling effect from being affected by the instability. This quadratic Stark shift has been observed, and exploited for the study of spin-3 Bose-Einstein condensates in the geometry  $\mathbf{E} \parallel \mathbf{B}$  [39] (where it was termed ‘‘quadratic Zeeman effect’’), but we are interested here in the geometric phases in the configuration  $\mathbf{E} \perp \mathbf{B}$ .

## IV. POSSIBLE ATOMIC INTERFEROMETER MEASUREMENT OF BERRY’S PHASES FOR SPINS WITH QUADRUPOLE COUPLING

Among several possible tests of the most striking results associated with the quadratic Stark coupling, there is an important goal which is to first observe the Berry’s phase generated by the rotation of  $\mathbf{E}$  around  $\mathbf{B}$ .

$$\beta(m = 0, \lambda) = - \oint p(0, \lambda) d\alpha. \quad (19)$$

This is one of the remarkable effects signalled out in Sec. II, that we expect to be large for  $S = 2$  when  $\lambda$  is close to 1, as highlighted by figure 1. The effect is particularly noteworthy for a spin larger than one, initially in an  $|S, 0\rangle$  substate, *i.e.* having its quantum averaged polarization

along  $\mathbf{B}$  cancelling out before an adiabatic cycle starts and after it stops. Therefore, the purpose of this section is to make precise suggestions for a measurement involving the rotation of  $\mathbf{E}$  around the orthogonal  $\mathbf{B}$  field, when both couplings, linear and quadratic, are of comparable magnitudes.

### A. Experimental compromises for spin-2 measurements with matter-wave interferometers.

Measurement of the phase difference acquired during the evolution of a quantum state requires a phase reference. Therefore the methods of matter-waves interferometry, first employed with neutron beams [44, 45], then adapted to magnetic resonance [21, 46] and now the subject of outstanding developments in cold atom physics [47], are especially well suited to observe Berry's phases. Atomic interferometry has been used before to measure a topological phase [48–52], but not in the case of a quadratic spin coupling, where the parameter space cannot be reduced to the surface of a sphere.

The initial atomic state is represented by a coherent superposition of two states having different energies, such as for instance two hf substates of an alkali atom. The main difficulty arises from the decay rate  $\Gamma_{dec} = \frac{\Omega^2}{\Delta_{2,1}^2} \Gamma_P$  (see section III.B Eq.(15)). For concreteness, we shall illustrate our proposal on the case of the two hf substates of  $^{87}\text{Rb}$ ,  $|F=1, m=0\rangle$  and  $|F=2, m=0\rangle$ . These have been chosen because first, only one of these two mixed substates acquires a Berry's phase; secondly, as we shall show, the range of parameters leading to  $\lambda \approx 1$  looks achievable for this isotope. By making a specific choice of the experimental parameters, we have found that an interferometer measurement of the peculiar features of the  $S=2, m=0$  Berry's phase is feasible within the present state of the art. However, as we shall see, there is actually little freedom for organizing the quantum cycle, if one wants to perform a measurement, free of non-adiabatic corrections.

#### i) Instability versus adiabatic requirements

The relevant range of the  $\lambda$  parameters ( $0 < \lambda \lesssim 1.5$ ), has to be reached with moderate laser intensities, in order to limit the decay rate of the dressed atoms. It requires the magnetic field to be small ( $\simeq 1$  mG), but not much smaller, in order to keep the field homogeneous over the atomic sample. The problem of the dressed atom losses would favour rapid quantum cycles but they should not spoil the validity the adiabatic approximation, in particular during the preparation of the coherent quantum state before it is submitted to the rotating electric field. It is then crucial to tame out the non-adiabatic oscillations generated by a linear ramping of  $\lambda(t)$  from zero to a value  $\simeq 1$ . An efficient remedy, given in [1], is to use a Blackman pulse-shape for the time derivative  $\dot{\lambda}(t)$  (See II.D)

As regards to the non-adiabatic correction associated with the angular velocity of the  $\mathbf{E}$  field rotation, they

are governed by the convenient parameter  $\eta = \dot{\alpha}/\gamma_s B$ . We have shown in our previous work [1] that all the corrections to the Berry's phase of the order  $\eta^{2n+1}$  vanish for  $n \geq 1$ , if  $\lambda(t)$  is given by the magic value  $\lambda^*(2, \eta(t))$  ( See Section IID.) We shall see that the set of values  $\eta = 0.3$  and  $\lambda^*(\eta) = 0.830$ , is an element of the overall compromise to be elaborated in the next subsection.

#### ii) Absence of quadrupolar light shift in the $F=1, m=0$ quantum state.

The cancellation of the quadratic light shift in the  $|1, 0\rangle$  quantum state of the  $^{87}\text{Rb}$  atom results from its absence of  $m = \pm 2$  sublevels. This simplifies the preparation of the coherent state which becomes a superposition of this unperturbed substate with the state perturbed by the laser field. This latter can be written  $|\Psi(2, 0; t=0)\rangle \equiv |\hat{\psi}(2, 0; \lambda(0))\rangle$  in the initial state of the quantum cycle; and is thus an eigenstate of  $\hat{H}(\mathbf{B}(t), \mathbf{E}(t))$  defined by Eq. (13). (Note that it is now useful to specify the spin value, since we are dealing with an admixture of two different hf states, hence belonging to different internal spin spaces).

#### iii) Parameter compromise for a simplified $S=2, m=0$ Berry's cycle performed on $^{87}\text{Rb}$ : one example.

Up to the end of this subsection and only here, we shall analyse the simplified  $S=2, m=0$  Berry's cycle defined by the boundary conditions:  $\lambda(0) = \lambda(T_c)$  and  $\alpha(T_c) - \alpha(0) = \pi$  and made the further assumptions  $\dot{\lambda}(t) = 0$  and  $\alpha(t) = \pi/T_c$ .

Table I presents the relevant parameters for  $^{87}\text{Rb}$ . For  $\Delta_{2,1} = \frac{1}{2}\Delta\mathcal{W}_P/\hbar = 2\pi \times 0.408$  GHz and  $\Omega = 2\pi \times 0.68$  MHz corresponding to a laser intensity of  $\approx 0.37$  mW/cm<sup>2</sup>, namely 0.113 times the “saturation” intensity,  $I_{sat}$  defined such that  $\Omega_{sat}^2 = \Gamma_P^2/8$ ; the quadrupolar Stark coupling,  $\Omega^2 g_F^2/\bar{\Delta}$ , amounts to  $2\pi \times 575$  Hz, while the linear Zeeman coupling is  $2\pi \times 700$  Hz/mG. In order to explore the interesting domain  $0.1 < \lambda \lesssim 1.5$ , the applied magnetic field should lie in the range  $10 \gtrsim B \gtrsim 0.65$  mG.

For constant angular velocity, the time needed to perform one quantum cycle is  $T_c = \pi/\dot{\alpha} = \pi/\eta\gamma_F B$ . If we want to keep the signal loss per cycle arising from the light-induced Stark coupling smaller than 1, the condition to be fulfilled is  $\Gamma_{dec} T_c \lesssim 1$ , or

$$\Gamma_{dec} T_c = \frac{\pi}{g_F^2} \frac{\lambda}{\eta} \frac{\bar{\Delta} \Gamma_P}{\Delta_{2,1}^2} = 4\pi \frac{\lambda}{\eta} \left( \frac{\Gamma_P}{2\pi\Delta\mathcal{W}_P} \right) \lesssim 1, \quad (20)$$

using Eq.(10 and 15). *Although the laser intensity is involved in both the expressions for  $T_c$  and  $\Gamma_{dec}$ , it disappears from  $\Gamma_{dec} T_c$ , but the intensity selected determines the magnetic field range and the minimum time needed for a measurement, which are interrelated together: the higher the field, the shorter the time. As noted before  $^{87}\text{Rb}$  is among alkali atoms the most favourable one with  $\Gamma_P/2\pi\Delta\mathcal{W}_P = 7 \times 10^{-3}$ . Therefore, one can only select the value of the ratio  $\lambda/\eta$ , preferably not exceeding a few units, for condition (20) to be satisfied. If one wishes to take advantage of the “magic” value property of  $\lambda$ , one is led to choosing a rotation speed of the  $\mathbf{E}$  field moder-*

TABLE I: Experimental parameters for a Berry’s phase measurement with  $^{87}\text{Rb}$  atoms supposing  $\Delta_{2,1} = -\Delta_{2,2}$ , and using time-independent “magic” conditions  $\eta = 0.3$ ,  $\lambda^*(\eta) = 0.83030$ . Values are given for two different laser intensities  $I$  expressed in terms of the “saturation” intensity  $I_{sat}$ , defined as  $\Omega_{sat}^2 = \Gamma_P^2/8$ . For the  $D_1$  line of Rb  $I_{sat} \approx 3.3 \text{ mW/cm}^2$ . The product  $\Gamma_{dec}T_c$  does not depend on  $I$  (see the text and Eq.(20)).

$\frac{\Delta_{2,1}}{2\pi\Delta\mathcal{W}_P}$	$\frac{\Delta_{2,2}}{2\pi\Delta\mathcal{W}_P}$	$\frac{\Delta}{2\pi\Delta\mathcal{W}_P}$	$\Gamma_{dec}T_c$	$100\frac{\Omega_P^2}{\Gamma_P^2}$	$I/I_{sat}$	$\gamma_F B^*(\text{s}^{-1})$	$\Gamma_{dec}(\text{s}^{-1})$	$T_c(\text{ms})$
0.5	-0.5	-0.25	0.244	1.4	0.113	4400	101	2.4
0.5	-0.5	-0.25	0.244	0.14	0.011	440	10.1	24

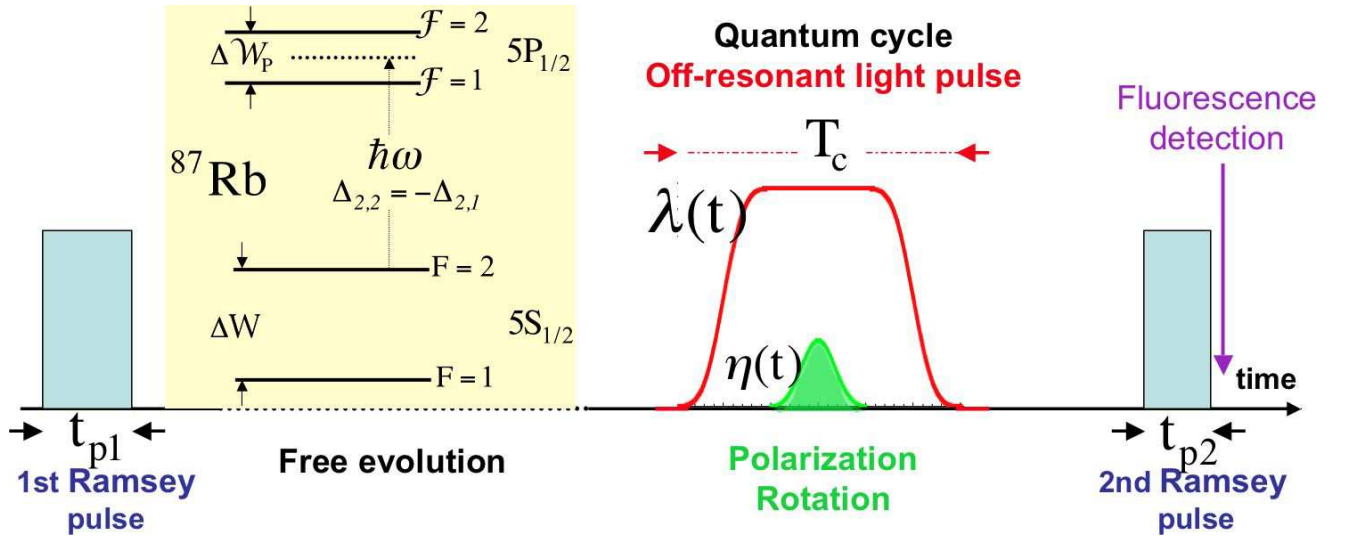


FIG. 3: (Color online) Interferometric measurement of the Berry’s phase for a spin 2 ( $m = 0$ ), chronology of the interferometric cycle including the quantum cycles, time in arbitrary units. The two phase-coherent Ramsey pulses are resonant for the  $1, 0 \rightarrow 2, 0$  transition of unperturbed  $^{87}\text{Rb}$  atoms. The quantum cycle of atoms in the state  $|2, 0\rangle$  starts with a ramping-up of the intensity of the off-resonant laser field, then, the rotation of its linear polarization starts smoothly towards a maximum angular speed. The whole operation is followed by the time reversed one to return to the initial state. The temporal dependences of both the light shift - normalized by the Zeeman shift,  $\lambda(t)$ - and the angular velocity of the polarization rotation - normalized by the Larmor precession angular frequency,  $\eta(t)$  - as well as their relative magnitudes are the parameters which govern the non-adiabatic corrections to the Berry’s phase in a critical way. By using Blackman pulses for both  $\dot{\lambda}(t)$  and  $\dot{\eta}(t)$  (“oscillation-taming”) and by satisfying the magic relation  $\lambda(t) = \lambda^*(\eta(t))$ , we show (see the text) how it is possible to keep these corrections well below the 0.1% level, with 40% of the initial cold-atom cloud surviving the light-induced decay. Insert: relevant atomic levels.

ately large, ( $\eta = 0.3$ ,  $\lambda^*(\eta)/\eta = 2.76$  for  $^{87}\text{Rb}$ ). Finally, this choice of experimental conditions (see Table I) leads to an acceptable signal loss for a single quantum cycle,  $\approx 24\%$ .

In the next subsection, we propose a realistic precise timing for the quantum cycle including now a discussion of the atomic loss during ramping up and down of the  $\lambda(t)$  parameter. This operation is of a critical importance to avoid non-adiabatic corrections.

## B. Towards an empirical determination of Berry’s phases, free of non-adiabatic corrections to the few 0.1 % level

### 1. Organization of the interferometric cycle

The interferometric cycle can be organized according to the method developed for high accuracy measurements with hfs measurements in cold atom atomic clocks to prepare the unperturbed coherent state  $\propto (|1, 0\rangle + c |2, 0\rangle)$  (e.g. [53]). Starting from the pure  $|1, 0\rangle$  state in pres-

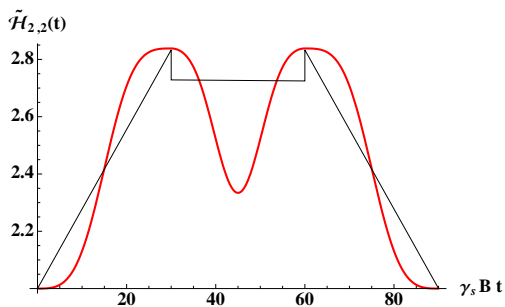


FIG. 4: (Color online) Time dependence of the diagonal ( $S = 2, m = 2$ ) matrix element of the Hamiltonian in the rotating frame, during the whole quantum cycle (time unit:  $(\gamma_s B)^{-1}$ ). Black curve: linear ramping for  $\lambda(t)$  and square pulse for  $\alpha(t)$ . Red curve: taming of the non-adiabatic oscillations (OT procedure) by using Blackman pulses for both  $\dot{\lambda}(t)$  and  $\dot{\alpha}(t)$ .

ence of  $\mathbf{B}$  and without the laser beam, hence without  $\mathbf{E}$ , one can use the Ramsey method [5] to prepare the unperturbed coherent state  $\propto (|1, 0\rangle + c|2, 0\rangle)$ , *i.e.* apply suddenly a short pulse (using either a rf field resonant for the  $|1, 0\rangle \rightarrow |2, 0\rangle$  frequency or two Raman pulses [54]). After a certain delay (time of free evolution,  $T$ , long compared to the durations of the rf pulses and the quantum cycle), the quantum cycle starts. The laser field responsible for  $\mathbf{E}$  is applied progressively and followed later on by the polarization rotation. It lasts for a duration  $T_c$ . Then, detection takes place. This consists in the application of a second Ramsey pulse, in presence of the  $\mathbf{B}$  field and without  $\mathbf{E}$ . The Berry's phase is obtained from the probability of finding the atoms in the  $|1, 0\rangle$  (and  $|2, 0\rangle$ ) state at the end of this pulse. The latter is measured by fluorescence detection following resonant excitation of the  $5S_{1/2, F=1} - 5P_{3/2, F=0}$  (and  $5S_{1/2, F=2} - 5P_{3/2, F=3}$ ) transitions. The cycle is depicted in Fig. 3

## 2. Implementing the quantum cycle via an oscillation-taming procedure

For clarity we suggest splitting the quantum cycle into three steps in which only one parameter at a time is varied. During the first and the last steps,  $\lambda$  alone is varied from 0 to  $\lambda_0$ , while during the second step  $\alpha$  is varied from 0 to  $\pi$ . Moreover, we decide to comply with the recommendation given and justified in [1] to satisfy the adiabatic approximation, for preparing the quantum state  $\Psi(2, 0; \lambda_0)$  at the beginning of step ii) with its polarization  $\langle S_z \rangle$  very close to its desired adiabatic value,  $p(2, 0; \lambda_0)$ . We avoid the discontinuities in the variation of  $\dot{\lambda}(t)$  by suitable tailoring of its shape:  $\lambda(t)$  will be assumed to be described by the primitive of a Blackman pulse. During step 2) the time variation of  $\dot{\alpha}$  is supposed to be represented by the Blackman function  $f(s)$  (Eq. 5); this is what we have termed the oscillation taming (OT)-procedure. In addition, it is advantageous and possible

to adjust  $\lambda(t)$  so that at any time it coincides with its “magic value” associated with the angular velocity  $\eta(t)$  at that time. This means that during steps i) and iii)  $\lambda_0$  is chosen equal to  $\lambda^*(0)$ , while during step ii), instead of keeping  $\lambda$  constant, we make a fine tuning of  $\lambda$  in order to satisfy Eq.(4). In practice, the variation of  $\lambda^*(\eta)$  in the range  $0 \leq \eta \leq 0.3$  is only half a percent of  $\lambda_0$ . The advantage of this strategy is the complete suppression of non-adiabatic corrections to the Berry's phase, which are odd under reversal of  $\dot{\alpha}$  (Sec.V.A), the even ones being suppressed by subtracting measurements for mirror-image cycles ( $\dot{\alpha}(t) \rightarrow -\dot{\alpha}(t)$ ).

Table II summarizes the chronology of Berry's cycle organized in three steps. For each step we give the expression the Hamiltonian  $\tilde{H}(t)$  acting within the frame rotating around the z axis with the angular velocity  $\dot{\alpha}$ , together with the time dependence of the parameters  $\lambda(t)$  and  $\eta(t)$ .

## 3. Quantitative predictions

Choosing  $T_c = 3\mathcal{T}$  which implies for the angular speed at its maximum  $\eta^{max} = 0.27$  (quite close to the value considered in Table I), we have simulated the exact time evolution. We have solved numerically the Schrödinger equation for the Hamiltonian represented by the sum of the three time dependent operators defined on the three successive time intervals. (Rounding-off theta functions are used to avoid discontinuities of higher order derivatives at the passage between two time-intervals.) The initial state at  $t = 0$  is the pure state  $|2, 0\rangle$ . If our attempt to create the conditions for the adiabatic approximation is working, we expect  $\langle S_z \rangle$  to be very close to its adiabatic value at the end of step i) and at the end of step ii). The calculation yields a difference of only 1 part in  $10^3$ . This indicates that, as anticipated from the discussion given in [1] (Sec.V.C), our implementation of the Berry's cycle leads to very small deviations from the strict adiabatic evolution, concerning the quantum states.

We have also probed the ability of this implementation to reproduce the adiabatic approximation as regards to the phase. We have performed two kinds of test. First we have calculated the phases of the final state for two mirror-image cycles ( $\dot{\alpha}(t) \rightarrow -\dot{\alpha}(t)$ ), still by solving numerically the Schrödinger equation, and compared their difference  $\Delta\Phi_D$  to the adiabatic Berry's phase, extracted by numerical evaluation of expressions (3). Our result,

$$\sin(\Delta\Phi_D - (\beta^+(2, 0; \lambda^*) - \beta^-(2, 0; \lambda^*))/2) = -0.000035, \quad (21)$$

is a good confirmation that, with the chosen timing, the corrections to the adiabatic approximation can be made exceedingly small. However, such an identity provides a determination of the Berry's phase only *modulo*  $\pi$ . Using the symmetry  $\beta^+(2, 0; \lambda^*) = -\beta^-(2, 0; \lambda^*)$ , the result of

TABLE II: Chronology of Berry's cycle organized in three equal steps using  $1/\gamma_s B$  as time unit. The function  $h(t)$  is the primitive of the Blackman function  $f(s)$  (Eq.(5)), varying between 0 and 1 over the unit time interval,  $h(t) = \int_0^t f(s)ds / \int_0^1 f(s)ds$ .

Time interval	$\tilde{\mathcal{H}}(t)$	$\lambda(t)$	$\eta(t) = \dot{\alpha}(t)/\gamma_s B$
step i) $0 \leq t \leq \mathcal{T}$	$S_z + \lambda(t)S_x^2$	$\lambda^*(0) h(t/\mathcal{T})$	0
step ii) $\mathcal{T} \leq t \leq 2\mathcal{T}$	$(1 - \eta(t))S_z + \lambda^*(\eta(t))S_x^2$	$\lambda^*(\eta(t))$ Eq.(4)	$\frac{\pi}{\gamma_s B \mathcal{T}} \dot{h} \left( \frac{t-\mathcal{T}}{\mathcal{T}} \right)$
step iii) $2\mathcal{T} \leq t \leq T_c = 3\mathcal{T}$	$S_z + \lambda(t)S_x^2$	$\lambda^*(0) h((T_c - t)/\mathcal{T})$	0

our calculation actually is:

$$\frac{1}{2}\Delta\Phi_D = \beta + \pi - 3.5 \times 10^{-5}. \quad (22)$$

The presence of  $\pi$  should not be considered as a surprise since our determination of the phase at the end of each cycle is obtained from the argument of the wave function, and is therefore defined *modulo*  $2\pi$ .

To remove the resulting ambiguity of  $\pi$  on the half-difference between mirror-image cycles, we have performed a second test. We compute the difference of the *adiabatic* phases,  $\Delta\Phi_{adiab}$  directly from the exact expression of the instantaneous eigenenergies of the  $|20; \lambda(t)\rangle$  state during the selected cycle, by doing well-defined quadratures. After comparison of both evaluations, the result

$$\frac{1}{2}\Delta\Phi_D = \frac{1}{2}\Delta\Phi_{adiab} + \pi - 2. \times 10^{-5} \quad (23)$$

merits two important remarks. First, the implementation of the quantum cycle that we have selected, succeeds to give an excellent control not only of the quantum state but also of the adiabatic phase. Second, the  $\pi$  increment appearing in our numerical evaluation of Eq.(22) confirms the fact that our theoretical evaluation of  $\Delta\phi_D$  is defined only *modulo*  $2\pi$ , as will also be the case for the experimental determination,  $\Delta\Phi_D^{exp}$ . But, at the same time, we obtain the means to remove the *modulo*  $\pi$  ambiguity in the determination of  $\beta$ : it is enough to look at the difference  $\frac{1}{2}(\Delta\Phi_D^{exp} - \Delta\Phi_{adiab})$  evaluated with a precision comparable to the experimental one. If, as we expect, this is found equal to an integer times  $\pi$  with enough accuracy (depending on the experimental precision, but better than 10 %), then the *modulo*  $\pi$  ambiguity is suppressed from  $\frac{1}{2}\Delta\Phi_D^{exp}$ .

Finally, the resulting empirical determination of the Berry's phase can be made free from systematic uncertainties caused by deviations from the adiabatic approximation, within an accuracy even beyond the 0.1% level. If we suppose that the time variation of  $\lambda$  is realized by adjusting the laser intensity while keeping the  $\mathbf{B}$  field constant  $\approx 1$  mG, the whole cycle duration amounts to  $\sim 15$  Larmor periods, *i.e.* 21 ms. Obviously, there is a

compromise between accuracy and duration: a faster  $\lambda$ -ramping could be employed but at the expense of lower accuracy.

#### 4. Interferometric detection of the Berry's phase

We can now present an explicit evaluation of the optical signal detected for a realistic choice of the parameters involved in the interferometric measurement. The Hamiltonian associated with the first rf pulse is written in the laboratory frame :

$$H_{lab}^{rf} = \frac{w\tau_3}{2} + \frac{1}{2}\omega_1 (\tau_- e^{iwt} + \tau_+ e^{-iwt}). \quad (24)$$

In this subsection we shall use a unit system such that  $\hbar = 1$  and we set  $w = 2\pi\Delta W$ . The symbols  $\tau_1, \tau_2, \tau_3$  stand for the familiar Pauli matrices and  $\tau_{\pm} = (\tau_1 \pm i\tau_2)/2$ . With these notations  $\omega_1$ , represents the coupling of the rf frequency field  $B_{rf}\hat{z}\sin wt$  with the magnetic dipole transition operator from the lower state  $|F = 1, m = 0\rangle$  to the upper state  $|F = 2, m = 0\rangle$ , and the mixed states are described by a two-component spinor  $\Psi(t) = \{X_2(t), X_1(t)\}$ . A straightforward computation performed within the frame rotating at the angular velocity  $w$  leads at the end of the first rf pulse ( $t = t_{p1}$ ) to the following state vector :

$$\tilde{\Psi}_{rot}(t_{p1}) = \{i \sin(\frac{\omega_1 t_{p1}}{2}), \cos(\frac{\omega_1 t_{p1}}{2})\}. \quad (25)$$

The value of  $\omega_1 t_{p1}$  will be specified later on. During the free evolution of duration  $T$ , the rf field is decoupled the rotating frame Hamiltonian vanishes, so that  $\tilde{\Psi}_{rot}(t_{p1} + T) = \tilde{\Psi}_{rot}(t_{p1})$ , when the quantum cycle starts. During the quantum cycle the spinor component  $X_2(t)$  acquires the phase  $\Phi_{20}^{\pm}$

$$\Phi_{20}^{\pm} = \Phi_D^{\pm} + \beta^{\pm}(20; \lambda^*), \quad (26)$$

the  $\pm$  index referring to the sign of  $\eta$ . Simultaneously, it is also affected by the light-induced decay, but  $X_1$  is not, so we obtain

$$\tilde{\Psi}_{rot}(t_{p1} + T + T_c) = \{i \sin(\frac{\omega_1 t_{p1}}{2}) \exp(-\bar{\Gamma}_{dec} T_c/2 + i\Phi_{20}), \cos(\frac{\omega_1 t_{p1}}{2})\}, \quad (27)$$

where  $\bar{\Gamma}_{dec}$  represents the decay rate averaged over the whole quantum cycle.

Up to now,  $\omega_1 t_{p_1}$  has been considered as a free parameter. It turns out to be advantageous to adjust it to make the two spinor components of equal magnitudes at the end of the quantum cycle. For this purpose, the condition to be satisfied is  $\tan(\omega_1 t_{p_1}/2) = \exp(\bar{\Gamma}_{dec} T_c/2) = 1.953$  in the present example, leading to  $\arctan \omega_1 t_{p_1}/2 = 1.0975$  rad, and a common magnitude of 0.455, instead of 0.707 when there is no decay. The signal loss resulting from the dressed atom instability is thus a factor 2.5.

A second  $\pi/2$  Ramsey pulse, can be applied to the state vector and be immediately followed by the detection process. The measured quantities are the probabilities  $\mathcal{P}_1$  and  $\mathcal{P}_2$  of finding the atom in states  $F = 1$  and  $F = 2$  respectively

$$\mathcal{P}_1 = \frac{1}{2}(1 - \cos \Phi_{20}^\pm) \quad (28)$$

$$\mathcal{P}_2 = \frac{1}{2}(1 + \cos \Phi_{20}^\pm). \quad (29)$$

After making the two measurements for  $\dot{\eta} > 0$  and  $\dot{\eta} < 0$  and using Eq. (26), one can extract  $2\beta(20; \lambda^*)$  modulo  $2\pi$ . We recall that the ambiguity of  $\pi$  appearing in this determination of  $\beta(20; \lambda^*)$  can be removed by combining this result with a calculation based on the knowledge of the eigenenergies. We see that, at the price of reducing the number of detected atoms by a factor 2.5, the fringe visibility can be kept very close to unity.

Subsections A and B mainly refered to cold alkali atoms or trapped alkali ions, offering integer spin values between 1 and 4. However, in the expanding family of laser cooled and trapped atoms there is the much less familiar case of chromium which, we believe deserves a special attention. ( See section III.C).

## V. BERRY'S PHASES FOR SPINS 3/2. POSSIBLE MEASUREMENTS

### A. Theoretical background

Although half-integer spins have no fully symmetric state like the  $m = 0$  substate of integer spins, their Berry's phases for quadratic Hamiltonians are interesting in their own right. With  $S=3/2$  we have the lowest spin state for which the dimension of the density matrix space exceeds that of the parameter space. In order to obtain a spin Hamiltonian able to generate the Aharonov-Anandan phase, one would have to include an octupole spin coupling. On the other hand, analytical Berry's phase formulas relative to the  $S = 3/2$  quadratic spin Hamiltonian have already been derived [29]. In Appendix B, we give explicit expressions for  $\mathcal{E}(m, \lambda)$  and the polarization  $p(m, \lambda)$  obtained by rewriting the results of ref [29] within the notations of [1] and the present paper. The results are displayed in Fig.5.

The most remarkable feature apparent in this figure concerns the level  $m = -\frac{1}{2}$ . The polarization  $p(-1/2, \lambda)$ , governing the size of Berry's phase, becomes  $\geq \frac{1}{2}$  for  $\lambda \geq 2$  indicating a strong mixing with the state  $m = \frac{3}{2}$ . At the same time, this level remains at a distance  $\simeq 1$  ( $\gamma_S B$  unit) from all other levels. This situation looks favourable for an empirical determination of Berry's phase  $\beta(\frac{3}{2}, -\frac{1}{2})$ . Moreover,  $\beta(\frac{3}{2}, -\frac{1}{2})$  differs widely from the spin one half Berry's phase  $\beta(\frac{1}{2}, -\frac{1}{2})$ . This difference provides the possibility of achieving a *maximum entanglement of three non-correlated spins* by the method described in section VI. of reference [1]. More details about this "holonomic" three Qbits entanglement are given in Appendix A.

### B. Possible measurements

There are two kinds of 3/2-spin systems for which measurements of Berry's phase might be considered : i) the  $^{35}\text{Cl}$  nuclei embedded inside a monocrystal matrix [21],[24] and ii) the  $^{201}\text{Hg}$  mercury isotope in a vapor [26] or a cold atom optical trap [53] (which could apply as well to odd isotopes of alkali-earths atoms like  $^{135}\text{Ba}$  and  $^{137}\text{Ba}$  placed in an optical dipole trap). Up to now in those systems, none of the experiments performed so far corresponds to what should be ideally realized for testing original features of Berry's phase.

The first experimental approach corresponds to the nuclear quadrupole resonance (NQR) of  $^{35}\text{Cl}$  nuclei ( $I=3/2$ ,  $\mu = 0.82 \mu_n$ ) of an oriented axially-symmetric single crystal of sodium chlorate put inside a sample rotor [21]. In this case, the quadratic spin coupling results from the interaction of the  $^{35}\text{Cl}$  nuclei quadrupole ( $Q = -0.08 \times 10^{-24} \text{cm}^2$ ) with the local axially-symmetric electric field gradient. However, up to now, measurements have been performed *only without* the linear coupling needed to lift the level-degeneracy. To investigate the interesting range  $\lambda \simeq 1$  the magnetic field  $\mathbf{B}$  (about 10 G) should be applied along the direction  $z$  of the first rotor axis [55], the quadrupolar axis of the rotating monocrystal being oriented perpendicularly to  $\mathbf{B}$ . The second rotor permits the precession of  $\mathbf{B}$  about the reference axis  $z$ . This set-up would be adequate for precise verifications of the Berry's phase and its non-adiabatic corrections.

In the second situation relative to  $^{201}\text{Hg}$ , the conditions corresponding to the hybrid "B-field laser-field" situation satisfying the  $\mathbf{E} \cdot \mathbf{B} = 0$  hypothesis, have been achieved in optical pumping experiments of early 1970's [26]. The quadratic spin coupling was adjusted as wanted over a large range of coupling ratios  $\lambda$ , (although there was no laser available at that time) but, though the applied fields were time-dependent, they were far from being applied adiabatically.

Measuring the Berry's phase could be performed by preparing  $^{201}\text{Hg}$  atoms in a coherent superposition of two Zeeman substates, the most interesting one being

$S=3/2$

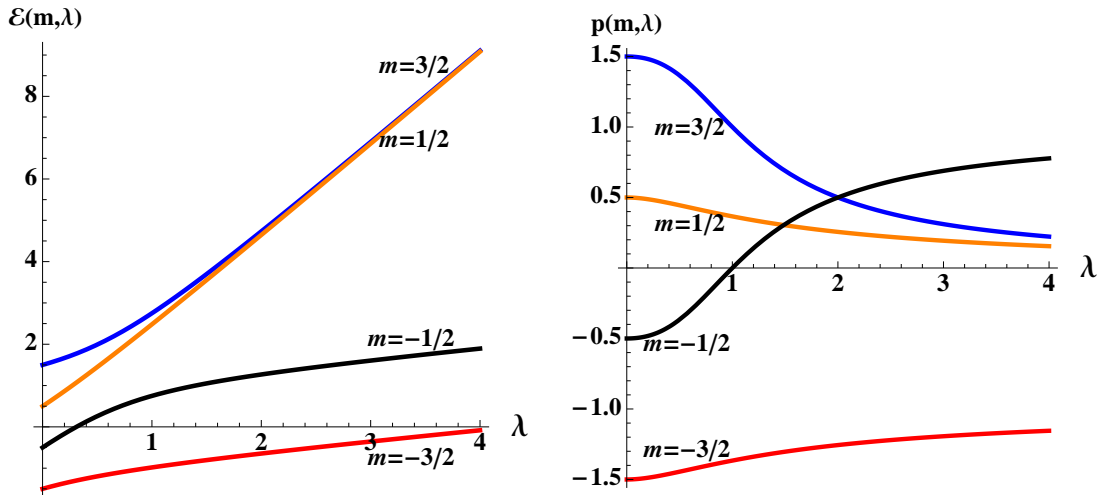


FIG. 5: (Color online) Reduced energies  $\mathcal{E}(m, \lambda)$  and polarization,  $p(m, \lambda)$  for  $S = 3/2$  within the interval  $0 \leq \lambda \leq 4$ . (The results for  $\lambda < 0$  are obtained by reflexion about the axes origin). The findings relative to the level  $m = -1/2$  for  $2 \leq \lambda \leq 4$  are quite remarkable. This level remains far away from the other ones and at the same times its polarization  $p(-1/2, \lambda)$ , giving the size of the Berry's phase, reaches values  $\geq 1$ . This indicates a strong mixing with the level  $m = 3/2$ .

$\Psi_{coh} = \frac{1}{\sqrt{2}}|3/2, -3/2\rangle + |3/2, -1/2\rangle$  for  $\lambda > 0$ . To this end one can start from the pure  $|F, m_F\rangle = |3/2, -3/2\rangle$  substate prepared by optical pumping and apply either a rf-frequency field or a pulsed modulated light beam to perform transverse optical pumping [26]. The fictitious electric field can be created using *adiabatic application* of a laser beam detuned from the hyperfine lines of the  $^1S_0 \rightarrow ^3P_1$  transition. The resulting ground-state instability will be mild compared with the case of  $^{87}\text{Rb}$  for two reasons. First, the *electron-Zeeman* coupling is replaced by the much smaller *nuclear-Zeeman* coupling, so that for a given detuning, much weaker radiation fields are needed to realize  $\lambda \approx 1$ . Secondly, the life time of the  $^3P_1$  Hg excited state is longer and the hfs splitting larger, allowing one to select a frequency detuning of a few gigahertz, the ratio  $\Gamma_P/\Delta\mathcal{W}_P$  is thus reduced by one hundred. Finally with all these parameters combining in a favourable way, in Hg the signal loss per cycle (Eq. (20)) becomes insignificant.

After one *adiabatic* quantum cycle, the phase shift induced by the time-dependence of  $\mathbf{E}$ , expected to be  $n_\alpha \pi(1 - p(-3/2, \lambda) + p(-1/2, \lambda))$  (Eq.(3)), is close to  $\pi$  over the range  $2 \leq \lambda \leq 4$ . There are several relevant signals: the modulation of a transmitted resonant probe pulse of low intensity at the frequency  $\gamma_F B \hbar^{-1}(\mathcal{E}(-1/2, \lambda) - \mathcal{E}(-3/2, \lambda))$  characteristic of the dressed atomic coherent state or the optical rotation of a linearly polarized beam tuned off-resonance of one hf component of the  $^1S_0 - ^3P_1$  transition. If the probe pulse is applied at the end of the quantum cycle, the quantity to be measured is the phase shift of this modulation

generated by the rotation of the  $\mathbf{E}$ -field. Since the sign of this shift changes with the direction of the rotation, making two consecutive measurements, with opposite rotation velocities, should yield the Berry's phase. When both results are combined, the *modulo*  $\pi$  ambiguity has to be resolved in the same way as indicated for the  $^{87}\text{Rb}$  interferometry experiment (cf. Sec. IV).

A different measurement scheme could exploit optical pumping with polarization modulated light, which can generate selectively high-order coherences [56, 57].

## VI. ANANDAN-AHARONOV GEOMETRIC PHASE FOR $S=1$

In this section we shall deal with the AA geometrical phase, still unobserved in the case of a spin-1. This phase is generated by quantum cycles along closed circuits drawn upon the space  $\mathbf{E}(\rho)$  of the pure state density matrices  $\rho(t) = |\Psi(t)\rangle\langle\Psi(t)|$ . During the cycle, at any instant  $t$ , the parallel transport condition:  $\langle\Psi(t)|\frac{d}{dt}\Psi(t)\rangle = 0$  has to be exactly satisfied. After considering the general form of the parallel transport Hamiltonian [28], we shall show that the hybrid B-field light-shift Hamiltonian can be tailored to suit to this form by adjusting the time-dependences of its parameters. This allows us to suggest a method for performing the measurement of the AA phase for spin-1, valid for example in the case of  $^{87}\text{Rb}$  atoms in the  $F = 1$  hf state.



### A. Aharonov-Anandan's versus Berry's phase as physical objects

In the spin-1 case the density matrix is completely determined by the knowledge of the polarization vector  $Tr(\rho(t)\mathbf{S})/\hbar$  and the ‘‘alignment’’ tensor  $A_{i,j} = Tr(\{S_i, S_j\})/\hbar^2$ . By performing an appropriate rotation upon the spin system  $R(t) = R(\hat{z}, \varphi(t)).R(\hat{y}, \theta(t)).R(\hat{z}, \alpha(t))$  involving the three Euler angles, the tensor  $A_{i,j}$  can be put under a diagonal form:  $\mathcal{A} = \hat{z} \otimes \hat{z} + \frac{1}{2}(1 + \sin \zeta) \hat{x} \otimes \hat{x} + \frac{1}{2}(1 - \sin \zeta) \hat{y} \otimes \hat{y}$  with the polarization lying along the z axis,  $\mathbf{p} = \cos(\zeta) \hat{z}$  where  $-\pi/2 < \zeta < \pi/2$ . The angle  $\zeta$ , together with the Euler angles, provide a system of coordinates for  $\mathbf{E}(\rho)$  which, by construction, is isomorphic to  $\mathbf{CP}^2$ . In Reference [28], G. Gibbons and one of us (CB), we have derived the explicit expression of the AA geometrical phase in terms of the above set of coordinates:

$$\beta_{AA} = \oint_{\mathcal{C}} \cos(\zeta) \cos(\theta) d\varphi - (1 - \cos(\zeta)) d\alpha. \quad (30)$$

The closed loop  $\mathcal{C}$  is specified by the following constraints within the time interval  $0 \leq t \leq T_c$ :  $\zeta(T_c) = \zeta(0)$ ,  $-\frac{\pi}{2} < \zeta(t) < \frac{\pi}{2}$ ,  $\theta(T_c) = \theta(0)$ ,  $0 < \theta(t) < \pi$  and  $\varphi(T_c) = \varphi(0) + 2n_\varphi\pi$ ,  $\alpha(T_c) = \alpha(0) + n_\alpha\pi$ , where  $n_\varphi$  and  $n_\alpha$  are non-vanishing integers. By setting  $\lambda = 2 \tan(\zeta)$  and using the method described in our previous work [1], one finds easily that Berry's phase for  $S = m = 1$ :  $\beta(1, 1) = \beta_{AA} \text{ mod}(2\pi)$ .

We would like to analyse the respective behaviour of  $\beta(1, 1)$  and  $\beta_{AA}$  in the limit  $\zeta = \frac{\pi}{2} + 0^-$  or equivalently  $\lambda \rightarrow +\infty$ . It is easily seen that our set of coordinates for  $\mathbf{CP}^2$  is singular for  $\zeta = \frac{\pi}{2}$ , since  $\mathbf{p}$  is vanishing and the alignment tensor  $\mathcal{A}$  reduces to  $\hat{z} \otimes \hat{z} + \hat{x} \otimes \hat{x}$ . Within such a density matrix configuration it is not possible to define the Euler angle  $\alpha$ ; this is like the longitude for spherical maps which is undefined at the north pole. However, the problem disappears when  $\zeta = \frac{\pi}{2} - \epsilon$ ,  $\epsilon$  being a small positive real, so that  $\beta_{AA}$ , which is designed to be free of non-adiabatic corrections, is well-defined by the closed loop integral (30), provided the conditions listed above be satisfied.

The case of Berry's phase is more delicate, since levels  $S = m = 1$  and  $S = 1, m = 0$  become degenerate in the limit  $\lambda \rightarrow +\infty$  and are already very close for  $\lambda > 2$ . As a typical example, let us consider the non-adiabatic correction  $\Delta\beta$  given by equation (73) of section V.C of [1]. It can be easily calculated in the present case:  $\Delta\beta = \int_0^{T_c} dt \mu^2 (\cos \theta \dot{\varphi} + \dot{\alpha}) p^{(2)}(1, \lambda)$  with  $p^{(2)}(1, \lambda) = \lambda + \mathcal{O}(1/\lambda^3)$ . The parameter  $\mu$ , governing the non-adiabatic effect is given by:  $\mu = -\sin \theta \dot{\varphi} / (\gamma_S B)$ . One sees clearly that the non adiabatic correction  $\Delta\beta$  is literally exploding when  $\lambda \rightarrow +\infty$ . Quite remarkably, the situation is very different in the limit  $\lambda \rightarrow -\infty$ : the separation between the levels  $S = m = 1$  and  $S = 1, m = 0$  grows like  $-\lambda$  and  $p^{(2)}(1, \lambda) = \mathcal{O}(1/\lambda^3)$ , so the non-adiabatic corrections can be ignored. Concerning the AA phase, there is practically no difference between the two

limits  $\zeta \rightarrow \pm\pi/2$ . The above results suggest that although  $\beta(1, 1)$  and  $\beta_{AA}$  are identical mathematical objects, their actual measurement will raise very different physical problems, as this will be confirmed in the following subsections.

### B. The spin-1 ‘‘parallel transport’’ Hamiltonian

In reference [28], we have constructed a Hamiltonian  $H_{\parallel}(t)$  which performs exactly a parallel transport around the closed circuit  $\mathcal{C}$  drawn upon  $\mathbf{CP}^2$ .  $H_{\parallel}(t)$  must satisfy at any time t, the parallel transport condition:  $\langle \Psi(t) | H_{\parallel}(t) | \Psi(t) \rangle \equiv Tr(\rho(t)H_{\parallel}(t)) = 0$ . In the present section, we shall limit ourselves, for the sake of simplicity, to closed circuits where  $\alpha(t)$  and  $\zeta(t)$  are the sole time dependent  $\mathbf{CP}^2$  coordinates. To proceed, it is convenient to introduce the ‘‘rotated’’ Hamiltonian:  $\hat{H}_{\parallel}(t) = U^\dagger(R(t))H_{\parallel}(t)U(R(t))$  with  $U(R(t)) = \exp(-\frac{i}{\hbar}S_z\alpha(t))$ . In reference [28], using equations (49) and (A5) it was found that  $\hat{H}_{\parallel}(t)$  takes the simple form:

$$\hat{H}_{\parallel}(t) = \frac{\dot{\zeta}(t)}{2\hbar} \{S_x, S_y\} - \frac{\dot{\alpha}(t)}{\hbar} \cos(\zeta(t))S_z^2 + \dot{\alpha}(t)S_z. \quad (31)$$

In the present context we are going to consider  $\hat{H}_{\parallel}(t)$  just as an ‘‘ansatz’’ and show that it does possess all the desired properties. To this end, we shall need the ‘‘rotating’’ frame Hamiltonian, which governs the evolution of  $\tilde{\Psi}(t) = U^\dagger(R(t))\Psi(t)$ :

$$\tilde{H}_{\parallel}(t) = \frac{1}{2\hbar} \dot{\zeta}(t) \{S_x, S_y\} - \frac{\dot{\alpha}(t)}{\hbar} \cos(\zeta(t))S_z^2. \quad (32)$$

From the identity:  $(S_x + iS_y)^2 - (S_x - iS_y)^2 = 2i\{S_x, S_y\}$ , it follows that  $\tilde{H}_{\parallel}(t)$  does not mix the state  $|1, m = 0\rangle$  with the states  $|1, m = \pm 1\rangle$ . As a consequence, if  $\tilde{\Psi}(t)$  satisfies the initial condition  $\tilde{\Psi}(0) = |1, 0\rangle$ , it can be written as a two-component wave function  $(\tilde{C}(1), \tilde{C}(-1))$ . Using standard text book formulas, it is then easily found that to derive its evolution one can replace, in  $\tilde{H}_{\parallel}(t)$ , the matrices  $\{S_x, S_y\} \hbar^{-2}$  and  $S_z^2 \hbar^{-2}$ , respectively by the Pauli matrix  $\sigma_y$  and the  $2 \times 2$  unit matrix. Exploiting the analogy with a Ramsey pulse, one arrives at the following expression for  $\tilde{\Psi}(t)$ :

$$\tilde{\Psi}(t) = (\cos(\frac{\zeta(t)}{2}), \sin(\frac{\zeta(t)}{2})) \exp -i \int_0^t d\alpha \cos(\zeta). \quad (33)$$

Using equations (31) and (33) one gets:  $\langle \tilde{\Psi}(t) | \hat{H}_{\parallel}(t) | \tilde{\Psi}(t) \rangle \equiv \langle \Psi(t) | H_{\parallel}(t) | \Psi(t) \rangle = 0$ . In other words, we have shown, as announced, that the Hamiltonian  $H_{\parallel}(t) = U(R(t))\hat{H}_{\parallel}(t)U^\dagger(R(t))$  performs a parallel transport along the particular closed circuit  $\mathcal{C}$  considered in this section. As a final check, let us calculate the AA phase in the laboratory frame. Writing  $\Psi(T_c) = \exp(-\frac{i}{\hbar}(\alpha(T_c) - \alpha(0))S_z) \tilde{\Psi}(T_c)$  and using the

phase shift  $\arg(\tilde{\Psi}(T_c)/\tilde{\Psi}(0))$ , deduced from equation (33), one arrives at the final expression for the AA phase:

$$\beta_{AA} = \int_0^{T_c} dt (\cos(\zeta) - 1)\dot{\alpha}(t), \quad (34)$$

which does agree, as expected, with the general formula giving (30) in the particular case  $\dot{\varphi} = 0$ .

### C. Parallel transport with a light-shift Hamiltonian

By adding to the Zeeman Hamiltonian the light-shift Hamiltonian  $\hat{H}_{ls}$  given by equation (8), for a beam polarization  $\hat{\epsilon} = \frac{1}{\sqrt{2}}(\hat{x} + \exp(i\chi)\hat{y})$ , one gets by a simple calculation a possible candidate for an experimental realization of  $\hat{H}_{\parallel}(t)$ :

$$\begin{aligned} \hat{H}_{exp} &= \gamma_S B S_z + \\ &+ W_{ls} \left( \sin(\chi) S_z + \frac{1}{2} \cos(\chi) \{S_x, S_y\} - \frac{1}{2} S_z^2 \right). \end{aligned} \quad (35)$$

Making the connection with the notations of section III:  $\chi = \pi/2 - 2\delta_e$  and  $\mathbf{S} = \hbar\mathbf{F}$ , we recognize Eq. (17) where we have dropped the c-number contribution which does not contribute to the geometric phase. By performing the identification:  $\hat{H}_{exp} \equiv \hat{H}_{\parallel}(t)$ , one obtains a set of three relations which open the road towards experimental realization of the spin-one AA phases:

$$\begin{aligned} \sin(2\delta_e) &= \frac{\dot{\zeta}}{2\dot{\alpha} \cos(\zeta)}, \\ W_{ls} &= 2\dot{\alpha} \cos(\zeta), \\ \gamma_S B &= \dot{\alpha} (1 - 2\cos(\zeta) \cos(2\delta_e)). \end{aligned} \quad (36)$$

We have found that physically satisfactory solutions of these equations do exist for the following simple realization of the closed circuit  $\mathcal{C}$ , within the time interval  $0 \leq t \leq T_c$ , namely

$$\zeta(t, T_c, \zeta_{max}) = 4\zeta_{max} \frac{t}{T_c} \left(1 - \frac{t}{T_c}\right), \quad \alpha(t, T_c) = n_\alpha \pi \frac{t}{T_c}, \quad (37)$$

with  $0 < \zeta_{max} < \pi/2$  and  $n_\alpha$  an arbitrary integer.

Figure 6 represents the three physical quantities which determine  $\hat{H}_{\parallel}(t)$ , in terms of the reduced time variable  $t/T_c$ , for two typical values of  $\zeta_{max}$ ,  $\pi/4$  and  $\pi/3$ . The first curve displays the angular variable  $\delta_e$ , which specifies the elliptical polarization of the light beam. The second and the third curves give in terms of the angular velocity  $\dot{\alpha}$ , respectively the ac Stark shift and the Larmor frequency associated with the external  $B$  field. Since we have chosen the angular velocity  $\dot{\alpha}$  time-independent the *total* magnetic field remains constant during the quantum cycle: the variation of the external field compensates the

effective light-field contribution (Eq. 36), therefore the total field does not vanish during the cycle.

One should keep in mind that the ac Stark shift introduces an instability of the the atomic ground state. For a particular detuning configuration, the instability of an alkali ground-state with  $I = 3/2$  can be accounted for by adding to  $\hat{H}_{exp}$  an anti-Hermitian operator proportional to the unit operator  $\mathbf{1}$ :  $\hat{H}_{exp} = \hat{H}_{\parallel}(t) - \frac{i}{2}\Gamma_{dec}\mathbf{1}$  with  $\Gamma_{dec} = 4 \frac{\Gamma_P}{2\pi\Delta\mathcal{W}_P} W_{ls}$ ,  $\Gamma_P$  and  $\Delta\mathcal{W}_P$  being the decay rate and the hyperfine splitting of the  $P_{1/2}$  state, (Eq.15). It is clear that such an instability does not affect the phase shift of the surviving atoms at the end of the quantum cycle. Using equation (36) and the explicit expression of the AA phase (34), one can calculate the average value of  $\Gamma_{dec}(t)$  over the AA cycle as follows:

$$T_c \langle \Gamma_{dec} \rangle = \int_0^{T_c} dt \Gamma_{dec}(t) = \frac{8\Gamma_P}{2\pi\Delta\mathcal{W}_P} (\beta_{AA} + n_\alpha \pi). \quad (38)$$

To end this section, we quote the values of the AA phases when  $\zeta_{max} = \pi/4$ ,  $\pi/3$  and  $n_\alpha = 1$  as well as the values of  $T_c \langle \Gamma_{dec} \rangle$  in the case of  $^{87}\text{Rb}$ ,

$$\begin{aligned} \zeta_{max} = \frac{\pi}{4} &\rightarrow \beta_{AA} = -0.4969, \quad T_c \langle \Gamma_{dec} \rangle = 0.148, \\ \zeta_{max} = \frac{\pi}{3} &\rightarrow \beta_{AA} = -0.8567, \quad T_c \langle \Gamma_{dec} \rangle = 0.128. \end{aligned} \quad (39)$$

As expected,  $\beta_{AA}$  is independent of the time scale  $T$ . The fact that this scaling property holds also for  $T_c \langle \Gamma_{dec} \rangle$  is less evident. There is a strong contrast with the case of Berry's phase measurement, where much higher atom losses are unavoidable if one wants to keep the non-adiabatic corrections below the 0.1% level.

### D. Realization of the parallel transport Hamiltonian on $^{87}\text{Rb}$ atoms

We suggest the realization of AA quantum cycles on spin-1 for the case of  $^{87}\text{Rb}$  atoms in the  $F = 1, m_F = 1$  hf state, when the sole time varying parameters are  $\zeta$  and  $\alpha$ . In practice this could be achieved by a well-orchestrated time-variation of the physical parameters  $W_{ls}(t)$ ,  $B(t)$ ,  $\delta_e(t)$  and  $\alpha(t)$  which characterize the B-field light-field configuration with  $\mathbf{B}$  colinear to the beam. Measurements can be done with a laser beam detuned midway from both hf components starting from the  $F = 1$  ground state ( $\Delta_{1,1} = -\Delta_{1,2} = 2\pi\Delta\mathcal{W}_P/2$ ) and with the magnitudes of  $B$  and  $W_{ls}$  adjusted for giving to both B- and E-couplings comparable magnitudes (see Fig. 6).

A precise interferometric measurement of the AA phase seems possible, the interferometric cycle being organized in a way very similar to the one described on Fig.3. Now, the first Ramsey pulse prepares a coherent superposition of  $F = 1, m_F = 1$ , submitted to the AA cycle, with the  $F = 2, m_F = 0$  state which serves as a reference. However, the features of the quantum cycle

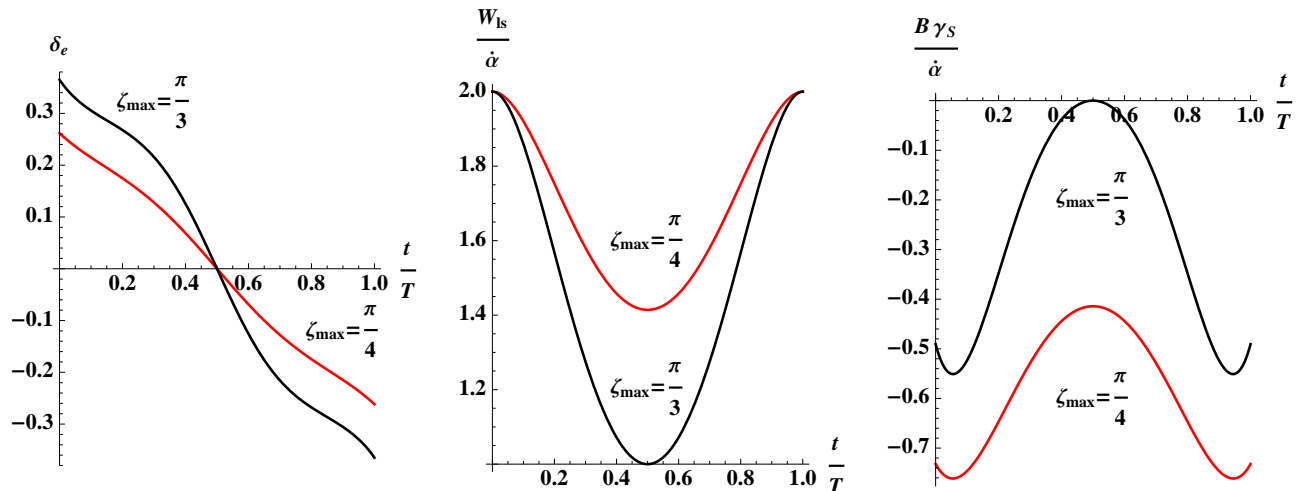


FIG. 6: (Color online) Time dependence of the physical parameters entering into the definition of the light-shift Hamiltonian which enables one to ensure parallel transport. The beam helicity is  $\cos 2\delta_e$ , its intensity, given by  $W_{ls}$ , Eq. (15), determines the magnitude of the quadrupolar Stark coupling and  $\gamma_S B + \cos 2\delta_e$  represents the linear dipole coupling, (for  $^{87}\text{Rb}$ ,  $F = 1$  atoms the beam has to be equally detuned from the two hf excited states). We assume the angular velocity constant and  $\zeta = \arctan(W_{ls}/2\gamma_S B) = 4\zeta_{max} \frac{t}{T}(1 - \frac{t}{T})$ .

itself will strongly differ, for comparable physical conditions (*i.e.* average field magnitude and light intensity). Instead of the progressive application of the time dependent Hamiltonian required for measuring Berry’s phase precisely, one can apply the “parallel transport” Hamiltonian *suddenly, without causing any alteration of the AA phase*. The total duration of the quantum cycle can thus be reduced by one order of magnitude. Thus, the atom loss during the quantum cycle is also greatly reduced.

To best illustrate the flexibility available in the choice of physical parameters allowing one to perform AA-cycles we end by a summary of the relations expressing how the cycle duration  $T_c$  is linked to the laser intensity averaged over one cycle on one hand, and to the effective magnetic field on the other hand (assuming the  $\zeta$  and  $\alpha$  time-dependences given by expressions (37), with  $\zeta_{max} = \pi/4$ ):

$$T_c \langle W_{ls} \rangle = 2(\beta_{AA} + \pi) = 5.28943, \quad (40)$$

$$\gamma_S B_{eff} T_c = \pi \quad (41)$$

In addition, we underline that, remarkably, *the atomic loss per cycle,  $T_c \langle \Gamma_{dec} \rangle$ , remains constant, whatever the absolute cycle duration* (see equation (38)).

## VII. SUMMARY AND PERSPECTIVES

The main purpose of the present paper is to suggest methods for measuring the Berry’s and AA quantum phases, in realistic experimental conditions, satisfying the physical requirements formulated in our theoretical work [1, 28, 29]. The spins are supposed to be nonlinearly coupled to time-dependent electromagnetic fields

(possibly effective ones) involving the simultaneous contributions of a linear and a quadrupole coupling. We have avoided the situations leading to degenerate eigenvalues, from which result non-Abelian Berry’s phases. Important simplifications in Berry’s phase calculation result from our assumption that the two effective fields involved, electric and magnetic, are orthogonal; as we have shown, the problem becomes then endowed with several symmetry properties which make it tractable for arbitrary spin values. However, Berry’s quantum cycles, performed in the Hamiltonian parameter space, require fulfilment of the adiabatic condition at any time of the spin evolution, a condition not easily satisfied in experiments on integer spin values  $> 1$  where the expected original features (Sec.II) deserve confrontation with our predictions. On the other hand, the AA phase is associated directly with a quantum cycle in the density matrix space. The so-called “parallel transport” condition is satisfied directly without the help of the the adiabatic approximation. The construction of the spin-1 “parallel transport” Hamiltonian - described in a simple case in section VI.B - is a rather difficult task. Instead of a fixed number of external physical parameters it involves  $4S$  parameters necessary to define a closed circuit in the density matrix space. This construction was performed initially in ref.[9] for spin  $S = \frac{1}{2}$  and, later on, in ref.[28] for  $S = 1$ , where the physical parameters involved are then the polarization vector and the alignment tensor. Detailed measurements have been performed in ref.[46] for spin  $S = \frac{1}{2}$  but no such investigation exists for  $S = 1$ . Our goal here has been to find how to go beyond the limitations encountered so far by experiments. To this end we describe concrete experimental situations, mainly chosen in the

field of atomic physics. We propose

- a realization of Berry’s cycles for spins  $> 1/2$  having quadrupole and dipolar couplings to external field with non-adiabatic correction below the 0.1% level.
- a realization of parallel transport quantum cycles on the spin  $S = 1$  density matrix leading to a measurement of the AA phase.

As seen in Sec.III, the total angular momentum of atoms in their ground state are good candidates for playing the role of isolated spins. For both Berry’s and AA cycles, a convenient experimental tool for coupling the spins non-linearly to external fields happens to be the “B-field light-shift” Hamiltonian. There are several variants: the quadrupolar coupling is realized thanks to the ac Stark shift induced by the linearly polarized light field, while a dipolar coupling of comparable magnitude can be ensured either by an external magnetic field (Eq.(13)) or the circular polarization of the light field (Eq.(17)). There is one drawback: the ac Stark shift induces an instability of the “dressed” ground state. The more severe problem lies in the fact that the quadrupole to dipole magnitude ratio  $\lambda$  acquires an imaginary part which invalidates the derivation of Berry’s phase given in ref. [1]. In the case of alkali atoms (say  $^{87}\text{Rb}$ ), we have found a simple remedy to get rid of this unwanted imaginary contribution: it is to tune the dressing beam frequency in such a way that the detunings  $\Delta_{21}$  and  $\Delta_{22}$  relative to the two transitions  $F = 1; 5S_{\frac{1}{2}} \rightarrow \mathcal{F} = 1, 2; 5P_{\frac{1}{2}}$  satisfy the simple relation  $\Delta_{21} + \Delta_{22} = 0$ . Concerning the instability of our isolated spin candidate, this puts a lower limit upon the duration of Berry’s quantum cycle which cannot be too short if one wishes to keep the non-adiabatic corrections below the level of 0.1%. A realistic proposal to solve this delicate problem is given in subsection IV.B.

To explore the still non-revealed Berry’s phase properties expected for a spin of two, remarkable in the case  $m = 0$ , we suggest (Sec.IV) a variant of a Ramsey interferometry experiment made on the clock transition of cold  $^{87}\text{Rb}$  atoms. Between the two Ramsey pulses the free evolution of a coherent superposition of the two  $m = 0$  hyperfine substates is interrupted by implementation of one quantum cycle in the upper state. The atoms interact with the off-resonant laser field, whose linear polarization rotates of  $\pi$  around  $\mathbf{B}$ . The cycle is organized in three steps i) the laser intensity is ramped up from 0 to its maximum, with its time-derivative tailored to fit a Blackman pulse; ii) the polarization is rotated with a time-dependent angular speed described by a Blackman pulse; fine tuning the laser intensity makes it possible to adjust the two-coupling ratio at its “magic” value depending on the instantaneous angular speed; iii) the laser intensity is ramped down to zero in the time-reversed way of step i). Measurement of the phase is repeated for the “mirror-image” cycle (opposite rotation speed), the half-difference is expected to provide the adiabatic Berry’s phase. We have simulated the experiment by performing the numerical resolution of the Schrödinger equation

in the rotating frame, allowing us to extract the value of the phase accumulated under the effect of the rotating E-field. We have found the result predicted by Berry’s phase expression with a deviation of only a few  $10^{-5}$ . We conclude that, within this chronology, the empirical determination of the Berry’s phase can be made free from any systematic uncertainty caused by deviations from the adiabatic approximation, within an accuracy well better than 0.1%. In addition, the selected timing contributes to minimize the cycle duration, once given the magnitude of non-adiabatic correction tolerated for one measurement. It is found that the problem raised by the state instability inherent to the light-induced quadratic coupling, is expected to cause only mild experimental difficulties.

As an example of Berry’s phase for half-integer spins we have chosen  $S = 3/2$ . Our predictions can be experimentally verified on  $^{201}\text{Hg}$  ground state atoms. For positive values of the quadrupole to dipole coupling ratio  $\lambda \simeq 2$ , the state  $S = 3/2, m = -1/2$  exhibits a large Berry’s phase in strong contrast with the  $S = 1/2, m = -1/2$  state behaviour. As seen in Sec.V and Appendix B, taking advantage of this  $S$ -dependence enables one to produce *maximum* entanglement between three initially non-correlated 1/2-Qbits in the state  $m = -1/2$ .

As Sec.VI demonstrates, our goal aiming at the exploration of AA cycles by realizing parallel transport of spins  $S = 1$  looks achievable. Thanks to precisely adjusted *time dependences of the light-shift Hamiltonian parameters*, (intensity, helicity of the beam, polarization rotation speed and magnitude of the magnetic field colinear to the light beam), it is possible to satisfy the parallel transport condition at any instant  $t$  of the cycle. As a result the trajectory followed by the spin-1 quantum state during its cyclic evolution is a closed loop composed of geodesic segments drawn on the spin-1 state space, *i.e.* the complex projective plane  $\mathbf{CP}^2$ . This provides new possibilities for exploring empirically the non-trivial geometrical properties of this four-dimensional space.

From a physical point of view, the main interest of the AA geometrical phase is that it could be generated by using as a  $S = 1$  candidate the  $F = 1$  hf level of the ground state of  $^{87}\text{Rb}$ , which is the building block of one of the most popular “optical” crystal. As for Berry’s phase there is a large flexibility available on the cycle duration provided correct scaling is applied to the other parameters, beam intensity and magnetic field. The advantage of the spin-1 AA phase compared to Berry’s is twofold.

- a. All limitations coming from the necessity of getting rid of the non adiabatic corrections disappear.
- b. The instability problem coming from the use of effective  $\mathbf{B}$ ,  $\mathbf{E}$  fields are much easier to control. This follows from the remarkable fact that the atom loss during the cycle duration  $T_c$  depends only on the value of the AA geometrical phase and not upon  $T_c$  (see equation (38)). For a typical value of  $\beta_{AA}$  the percentage of atom loss per cycle is about 15%.

In the present paper we have dealt, for sake of simplicity, only with cycles involving  $\alpha$  and  $\lambda$  as time-dependent coordinates. The construction of a parallel transport Hamiltonian can be extended to an arbitrary closed circuit of  $CP^2$ , using the results of reference [28].

### Appendix A: Entanglement of three non-correlated one-half spins using Berry's quantum cycles

Adapting the method of reference [1], we introduce the three non-corellated spin states with  $M = \sum_{i=1}^3 m_i = \frac{1}{2}$ :

$$\Phi^{(1)} = |-\frac{1}{2}\rangle \otimes |\frac{1}{2}\rangle \otimes |\frac{1}{2}\rangle, \quad (\text{A1})$$

$\Phi^{(2)}$  and  $\Phi^{(3)}$  being obtained by a circular permutation of the  $m_i$ . These three states form an orthogonal basis for the set of three one half-spin states with  $M = \frac{1}{2}$ . The next step is to construct three orthogonal eigenstates of  $\mathbf{S}^2$  with  $\mathbf{S} = \sum_{i=1}^3 \mathbf{s}_i$  which are linear combination of the  $\Phi^{(i)}$ . Using the rules of addition of quantum angular momenta, one finds that the possible eigenvalues of  $\mathbf{S}^2$ ,  $\hbar^2 S(S+1)$ , correspond to  $S = \frac{3}{2}$  and  $S = \frac{1}{2}$ . There is a unique way to construct the state  $S = \frac{3}{2}$ : one applies the operator  $S_- = S_x - iS_y$  upon the state  $S = M = \frac{3}{2}$ , i.e.  $\Psi_{\frac{3}{2}\frac{1}{2}} = |\frac{1}{2}\rangle \otimes |\frac{1}{2}\rangle \otimes |\frac{1}{2}\rangle$ . One obtains immediately:

$$\Psi_{\frac{3}{2}\frac{1}{2}} = \frac{1}{\sqrt{3}}(\Phi^{(1)} + \Phi^{(2)} + \Phi^{(3)}). \quad (\text{A2})$$

This state is invariant under all permutations of the 3-spin states. One has now to construct two orthogonal states with  $S = M = \frac{1}{2}$ , denoted  $\Psi_{\frac{1}{2}\frac{1}{2}}^n$ , ( $n = 1, 2$ ), which differ by their symmetry under the permutations of the three spins. Ignoring for a moment the orthogonality condition, it is easy to obtain two such states, linearly independent,  $\Phi^{(1,j)} = (\Phi^{(1)} - \Phi^{(j)})/\sqrt{2}$  with  $j = 2, 3$ . By introducing in  $\Phi^{(1,j)}$  the explicit expression of the states  $\Phi^{(j)}$ , one finds, by applying the rising operator  $S_+ = S_x + iS_y$ , that indeed,  $S_+ \Phi^{(1,j)} = 0$ . It is then easily seen that two orthogonal states  $\Psi_{\frac{1}{2}\frac{1}{2}}^n$  are given, up to a normalization factor, by the sum and the difference  $\Phi^{(1,2)} \pm \Phi^{(1,3)}$ :

$$\Psi_{\frac{1}{2}\frac{1}{2}}^1 = \frac{1}{\sqrt{6}}(2\Phi^{(1)} - \Phi^{(2)} - \Phi^{(3)}); \Psi_{\frac{1}{2}\frac{1}{2}}^2 = \frac{1}{\sqrt{2}}(\Phi^{(2)} - \Phi^{(3)}). \quad (\text{A3})$$

It is now a matter of simple algebra to write the non-correlated state  $\Phi^{(1)}$  as a linear combination of the three above angular momentum eigenstates:

$$\Phi^{(1)} = \frac{1}{\sqrt{3}}(\Psi_{\frac{3}{2}\frac{1}{2}} + \sqrt{2}\Psi_{\frac{1}{2}\frac{1}{2}}^1) \quad (\text{A4})$$

An important feature of the three states  $\Psi_{\frac{3}{2}\frac{1}{2}}$ ,  $\Psi_{\frac{1}{2}\frac{1}{2}}^1$ ,  $\Psi_{\frac{1}{2}\frac{1}{2}}^2$  is their symmetry properties under permutations of the three spins. Let us introduce

the fully symmetric operator  $\mathcal{S} = \frac{1}{6} \sum_{i=1}^6 p_i$  where  $p_i$  is one of the 6 possible permutations of the three  $m_i$ . It is then easily verified that:  $\mathcal{S} \Psi_{\frac{3}{2}\frac{1}{2}} = \Psi_{\frac{3}{2}\frac{1}{2}}$  while  $\mathcal{S} \Psi_{\frac{1}{2}\frac{1}{2}}^n = 0$ . On the other hand, the permutation (23) applied upon the two  $S = \frac{1}{2}$  states gives: (23)  $\Psi_{\frac{1}{2}\frac{1}{2}}^1 = \Psi_{\frac{1}{2}\frac{1}{2}}^2$  and (23)  $\Psi_{\frac{1}{2}\frac{1}{2}}^2 = -\Psi_{\frac{1}{2}\frac{1}{2}}^1$ .

We are going to study the adiabatic evolution of the three non-correlated, 1/2 spin states governed by  $H_3(t) = H(\mathbf{B}(t), \mathbf{E}(t))$ , which looks formally like the quadratic spin Hamiltonian of Eq.(1) discussed extensively in the present paper, but with a crucial difference lying in the fact that  $\mathbf{S}$  is meant to be the total spin operator  $\mathbf{S} = \sum_{i=1}^3 \mathbf{s}_i$ . The Hamiltonian  $H_3(t)$  is invariant under all the the permutations of the three spins and, as a consequence, all its non-diagonal matrix elements taken between any pair of the three above states are vanishing. The above result can be extended to the set of three states  $\Psi_{\frac{3}{2}M}$ ,  $\Psi_{\frac{1}{2}M'}$  with  $|M| = |M'| = \frac{1}{2}$  obtained by application of the raising (lowering) operators  $S_{\pm} = S_x \pm iS_y$ , also permutation invariant. We are then lead to the conclusion [1] that *the three states  $\Psi_{\frac{3}{2}M}$ ,  $\Psi_{\frac{1}{2}M'}$  behave vis à vis the Hamiltonian  $H_3(t)$ , as if they were associated with isolated spins  $S$ .*

Our Berry's cycle would be organized in a way similar to the one we described in section IV of the present paper, but with one difference: the precession Euler angle  $\varphi$  has to be among the cyclic parameter in order to have a non vanishing Berry's phase for  $S = \frac{1}{2}$ . Otherwise it would be impossible to achieve a maximum entanglement. As an illustration, we shall consider situations where during the  $\varphi$ -cycles  $\theta$  and  $\lambda$  have predefined fixed values obtained by adiabatic ramping processes, analogue to those discussed in [1]. It is then convenient to introduce the difference  $\Delta\beta(\lambda, \theta)$  between the  $S = \frac{3}{2}$  and  $S = \frac{1}{2}$  Berry's phases:  $\Delta\beta(\lambda, \theta) = \cos \theta (p(\frac{3}{2}, \frac{1}{2}; \lambda) - \frac{1}{2}) 2n_\varphi \pi$ .

At the end of the Berry's cycle, the initial non-correlated state  $\Phi^{(1)}$ , written as a linear combination of angular states behaving as isolated spin systems, has evolved into the following state:

$$\begin{aligned} \Phi_{BP}^{(1)}(\lambda) &= \exp(i\beta(\frac{3}{2}, \frac{1}{2}; \lambda)) \frac{1}{\sqrt{3}} \Psi_{\frac{3}{2}\frac{1}{2}} + \\ &\quad \sqrt{\frac{2}{3}} \exp(i\beta(\frac{1}{2}, \frac{1}{2}; \lambda)) \Psi_{\frac{1}{2}\frac{1}{2}}^1. \end{aligned} \quad (\text{A5})$$

We rewrite the right-hand side of the above equation in terms of the non-correlated states  $\Phi^{(i)}$ , and factor out the overall phase  $\chi = \beta(\frac{3}{2}, \frac{1}{2}, \lambda)$  in order to exhibit the Berry's phase difference  $\Delta\beta = \beta(\frac{3}{2}, \frac{1}{2}, \lambda) - \beta(\frac{1}{2}, \frac{1}{2}, \lambda)$ . We get the final expression for our candidate for a three one half-spin entangled state:

$$\begin{aligned} \Phi_{BP}^{(1)}(\lambda) &= \frac{\exp i\chi}{3} ((1 + 2 \exp(-i\Delta\beta))\Phi(1) + \\ &\quad (1 - \exp(-i\Delta\beta))(\Phi(2) - \Phi(3))). \end{aligned} \quad (\text{A6})$$

To achieve a maximum entanglement one must impose the equality of the absolute values of the two mixing co-

efficients,  $|1 + 2 \exp(-i\Delta\beta)| = |1 - \exp(-i\Delta\beta)|$ . It is easily found that this implies the condition  $\Delta\beta = \pm \frac{2\pi}{3}$ . To get explicit results, we have chosen the typical case  $n_\varphi = 2$  and  $\theta = \frac{2\pi}{3}$ . Using equation (B2) of Appendix B, one gets the following value for  $\lambda_{max} = -0.784562$ . This negative value is welcome because it allows one to avoid the near-crossing of the two levels  $\mathcal{E}(\frac{3}{2}, \frac{3}{2}, \lambda)$  and  $\mathcal{E}(\frac{3}{2}, \frac{1}{2}, \lambda)$  which occurs for  $\lambda \gtrsim 1$ . For  $n_\varphi = 2$  and  $\theta = \frac{2\pi}{3}$  the  $S = \frac{1}{2}$  Berry's phase takes the simple value:  $\beta(\frac{1}{2}, \frac{1}{2}) = \pi \text{ mod}(2\pi)$ , since we know  $\Delta\beta$ , this leads to  $\beta(\frac{3}{2}, \frac{1}{2}, \lambda_{max}) = -\frac{\pi}{3} \text{ mod}(2\pi)$  and to the final form

$$\begin{aligned} \Phi_{BP}^{(1)}(\lambda_{max}) = & \frac{1}{\sqrt{3}}(-\exp(i\frac{\pi}{6})|-\frac{1}{2}\rangle \otimes |\frac{1}{2}\rangle \otimes |\frac{1}{2}\rangle \\ & + \exp(-i\frac{\pi}{6})|\frac{1}{2}\rangle \otimes |-\frac{1}{2}\rangle \otimes |\frac{1}{2}\rangle \\ & - \exp(-i\frac{\pi}{6})|\frac{1}{2}\rangle \otimes |\frac{1}{2}\rangle \otimes |-\frac{1}{2}\rangle). \end{aligned} \quad (\text{A7})$$

The initial non-correlated state  $\Phi^{(1)}$  has been transformed, at the end of this specially designed Berry's cycle, into a correlated state with a maximum entanglement.

### Appendix B: Berry's phase quantum cycles generated by $S = 3/2$ non linear Hamiltonians

We give here basic formulas for the Berry phases relative to a spin  $S = \frac{3}{2}$ . They have been adapted from

reference [29] in order to make them compatible with the notations of the present paper. We begin by the reduced Hamiltonians  $\mathcal{H}_{even}$  and  $\mathcal{H}_{odd}$  connecting states with  $(-1)^{3/2-m} = \pm 1$  respectively:

$$\begin{aligned} \mathcal{H}_{even}(3/2, \lambda) &= \begin{pmatrix} \frac{3\lambda}{4} + \frac{3}{2} & \frac{\sqrt{3}\lambda}{2} \\ \frac{\sqrt{3}\lambda}{2} & \frac{7\lambda}{4} - \frac{1}{2} \end{pmatrix} \\ \mathcal{H}_{odd}(3/2, \lambda) &= \begin{pmatrix} \frac{7\lambda}{4} + \frac{1}{2} & \frac{\sqrt{3}\lambda}{2} \\ \frac{\sqrt{3}\lambda}{2} & \frac{3\lambda}{4} - \frac{3}{2} \end{pmatrix} \end{aligned} \quad (\text{B1})$$

From them one gets readily the explicit values of  $\mathcal{E}(m, \lambda)$  and  $p(m, \lambda)$  for  $m = \frac{3}{2}$  and  $m = \frac{1}{2}$ .

$$\begin{aligned} \mathcal{E}(3/2, \lambda) &= \frac{1}{4} \left( 4\sqrt{\lambda^2 - \lambda + 1} + 5\lambda + 2 \right) \\ p(3/2, \lambda) &= \frac{2 - \lambda}{2\sqrt{\lambda^2 - \lambda + 1}} + 1/2 \\ \mathcal{E}(1/2, \lambda) &= \frac{1}{4} \left( 4\sqrt{\lambda^2 + \lambda + 1} + 5\lambda - 2 \right) \\ p(1/2, \lambda) &= \frac{\lambda + 2}{2\sqrt{\lambda^2 - \lambda + 1}} - 1/2 \end{aligned} \quad (\text{B2})$$

The formulas for  $m < 0$  are easily obtained from the reflexion law derived in [1] section III:

$$\mathcal{E}(-m, \lambda) = -\mathcal{E}(m, -\lambda), \quad p(-m, \lambda) = -p(m, -\lambda).$$

- 
- [1] M.A. Bouchiat and C. Bouchiat, J. Phys. A: Math. Theor. **43**, 465302 (2010). arXiv:1006.2528
- [2] T. Eguchi and P.G.O Freund, Phys.Rev. Lett. **37**, 1251 (1977).
- [3] G.W. Gibbons and C.N. Pope, Commun. Math.Phys. **61**, 239 (1978).
- [4] G.W. Gibbons and S.W. Hawking, Commun. Math.Phys. **66**, 291 (1979).
- [5] N. F. Ramsey, Phys. Rev. **76**, 996L. and *Molecular Beams* (Clarendon, Oxford, UK, 1956), pp. 124-133 (1949).
- [6] M.V. Berry, Proc. R. Lond. A392, 45 (1984).
- [7] B. Simon, Phys. Rev. Lett. **51**, 2167 (1983).
- [8] Y. Aharonov and D. Bohm, Phys. Rev. **115**, 485 (1959).
- [9] Y. Aharonov and J. Anandan, Phys. Rev. Lett. **58**, 1593 (1987).
- [10] A. Shapere and F. Wilczek, *Geometric Berry's Phases in Physics*, Advanced Series in Mathematical Physics, Vol. 5 (World Scientific, Singapore) (1989).
- [11] J. Anandan, J. Christian and K. Wanelik, Resource letter GPP-1 *Geometric phases in physics*, Am. J. Phys. **65**, 180 (1997).
- [12] M. Berry, Sci. Am. **259**, 46 (1988).
- [13] Holstein, J. Am. Phys. **57**, 1079 (1989).
- [14] J. Zwanziger, M. Koenig and A. Pines, Ann. Rev. Phys. Chem. **41**, 601 (1990).
- [15] E. Sjöqvist, Physics **1**, 35 (2008).
- [16] J. A. Jones, V. Vedral, A. Ekert, and G. Castagnoli, Nature **403**, 869 (2000).
- [17] E.D. Commins, Am. J. Phys. **59**, 1077 (1991).
- [18] M. Pendlebury *et al.*, Phys. Rev. A **70**, 032102 (2004).
- [19] DeKieviet *et al.*, 2010, e-print arXiv:physics.atom-ph/1003.0622.
- [20] E.R. Meyer, *et al.*, Phys. Rev. A, **80**, 062110 (2009).
- [21] R. Tycko, Phys. Rev. Lett. **58**, 2281 (1987).
- [22] F. Wilczek and A. Zee, Phys.Rev.Lett, **58**, 2111 (1984).
- [23] A. Zee, Phys. Rev. A **38**, 1 (1988).
- [24] J.W. Zwanziger, M. Koenig and A. Pines, Phys. Rev. A **42**, 3107 (1990).
- [25] F. Wilczek and A. Zee, Phys. Rev. Lett. **38**, 1 (1988).
- [26] C. Cohen Tannoudji and J. Dupont-Roc, Phys. Rev. A **5**, 968 (1972).
- [27] C. Cohen Tannoudji, J. Dupont-Roc and G. Grynberg, *Atom-Photon Interactions* (Wiley, New York, 1992).
- [28] C. Bouchiat and G. W. Gibbons, J. Phys. France **49**, 187 (1988).
- [29] C. Bouchiat, J. Phys. France **50**, 1041 (1989).
- [30] M. Kitagawa and M. Ueda, Phys. Rev. A, **47**, 5138 (1993).
- [31] A. Sorensen, L.-M. Duan, J. I. Cirac and P. Zoller, Nature **409**, 63 (2001) and references therein.
- [32] M.A. Bouchiat and C. Bouchiat, in preparation.
- [33] Xi Chen, J. Lizuain, A. Ruschaupt, D. Guéry-Odelin, J.G. Muga, Phys. Rev. Lett. **105**, 123003 (2010) and references therein.

- [34] F. J. Harris, Proc. IEEE, **66**, 51 (1978).
- [35] P.G.H. Sandars, Proc. Phys. Soc. London, **92**, 857 (1967); J.R.P. Angel and P.G.H. Sandars, 1968, Proc. R. Soc. London, Ser. A **305**, 125.
- [36] C. Ospelkaus, U. Rasbach, and A. Weis, Phys. Rev. A **67**, 011402 (2003); S. Ulzega *et al.*, Europhys. Lett. **76** 1074 (2006) and **78** 69901 (2007).
- [37] H. Gould, E. Lipworth and M.C. Weisskopf, Phys. Rev. **188**, 24 (1968).
- [38] C.C. Bradley *et al.*, Phys. Rev. A **61** 053407 (2000).
- [39] L. Santos *et al.*, Phys. Rev. A **75**, 053606 (2007).
- [40] Q. Beaufils *et al.*, Phys. Rev. A **77**, 061601(R) (2008).
- [41] M.A. Bouchiat, J. Physique **26**, 415 (1965).
- [42] The irreducible tensor decomposition of the dipole coupling (Eq.11) for alkalis lightened by a beam close to resonance with the  $D_1$  transition has been derived long ago [41], together with the relation between the Stokes parameters of the light beam and the tensor components of the atom angular momentum. The interest of these relations which have been frequently used for interpreting optical pumping experiments, has been recently re-asserted in the context of quantum control of atomic spins in polarization spectroscopy, *e.g.* I. H. Deutsch and P.S. Jesssen, Opt. Commun. **283** 681 (2010).
- [43] R.F. Gutterres *et al.*, Phys. Rev. A **66**, 024502 (2002).
- [44] U. Bonse and H. Rauch, *Neutron interferometry* (Oxford Univ. Press. , 1979) pp. 124-133.
- [45] T. Bitter and D. Dubbers, Phys. Rev. Lett. **59**, 251 (1987).
- [46] D. Suter, K.T. Mueller and A. Pines, 1988, Phys. Rev. Lett. **60**, 1218.
- [47] P. Berman, *Atomic Interferometry* (Academic Press, San Diego, 1997).
- [48] K. Sangster *et al.*, Phys. Rev. Lett., **71**, 3641 (1993).
- [49] K. Zeiske *et al.*, Appl. Phys. B, **60**, 205 (1995).
- [50] A. Görlitz, B. Schuh and A. Weis, Phys. Rev. A **51**, R4305 (1995).
- [51] J. Skalla and G. Wäckerle, Appl. Phys. B **64**, 459 (1997).
- [52] C.L. Webb *et al.*, Phys. Rev. A **60**, R1783 (1999).
- [53] S. Bize *et al.*, Europhys. Lett. **45**, 558 (1999).
- [54] M. Kasevich and S. Chu, Phys. Rev. Lett. **67**, 181 (1991).
- [55] A. Samoson and A. Pines, Rev. Sci. Instrum., **60**, 3239 (1989).
- [56] V.V.Yashchuk *et al.*, Phys. Rev. Lett., **90**, 253001 (2002).
- [57] D. Budker *et al.*, Rev. Mod. Phys., **74**, 1153 (2002).